

SLOPE STABILITY CASE STUDY BY LIMIT
EQUILIBRIUM AND NUMERICAL METHODS

By

OMAR ALI M. MOUDABEL

Bachelor of civil Engineering

Tripoli University

Tripoli, Libya

1997

Submitted to the Faculty of the
Graduate College of the
Oklahoma State University
in partial fulfillment of
the requirements for
the Degree of
MASTER OF SCIENCE
May, 2013

SLOPE STABILITY CASE STUDY BY LIMIT
EQUILIBRIUM AND NUMERICAL METHODS

Thesis Approved:

Dr. Xiaoming Yang

Thesis Adviser

Dr. Garry H. Gregory

Dr. Stephen A. Cross

Name: OMAR ALI M MOUDABEL

Date of Degree: MAY, 2013

Title of Study: SLOPE STABILITY CASE STUDY BY LIMIT EQUILIBRIUM AND
NUMERICAL METHODS

Major Field: CIVIL ENGINEERING

ABSTRACT:

Stability analysis of slopes susceptible to different types of failures can be performed with different techniques. The selection of an appropriate technique is, therefore, a very important process of slope stability evaluation. In the assessment of slopes, the factor of safety values still remain the primary index for determining how close or how far slopes are from failure. Traditional limit-equilibrium (LEM) techniques are the most commonly-used analysis methods. Recently, however, the significant computing and memory resources typically available to geotechnical engineers, combined with low costs, have made the Finite Element Method (FEM) or Finite Difference Method (FDM) a viable additional method of analysis. The Shear Strength Reduction (SSR) technique enables FEM or FDM to calculate factors of safety of slopes.

In this study, five real case studies that used the Spencer's method, Morgenstern and Price's method, and finite difference method by SSR. The Spencer's and Morgenstern & Price's methods are limit equilibrium methods that satisfy all the static equilibrium condition. On the other hand, FEM or FDM methods are based on SSR. Slope stability of these five different cases was analyzed using LEM and FDM methods. GEOSTASE[®] software was used for analysis based on LEM, and FLAC[®] software was used for analysis based on FDM. Factors of safety (FS) values were calculated using both methods, and the results were compared for their applicability. Based on the comparison results, conclusions were drawn on the application of these methods. It was found that the results from these two methods are generally in good agreement. However, it was found in some cases that FDM analysis gave a factor of safety value that was less than the values determined by LEM. This is because the FDM considers more parameters and performs a detailed analysis of stress and strain conditions in the strata under consideration. Although the results may be different, the synergism of both methods can give valuable source of check on the slope failure mechanism.

TABLE OF CONTENTS

Chapter	Page
CHAPTER I: 1. INTRODUCTION	1
1.1 Background	1
1.2 Objectives	2
1.3 Methodology	3
1.4 Organization of the Thesis	3
CHAPTER II: 2. LITERATURE REVIEW	4
2.1 Introduction	4
2.2 Types of Slope Failures and Instability Mechanism	4
2.3 Shear Failure and Mohr-Coulomb Model Description	7
2.4 Limit Equilibrium Method	8
2.4.1 Spencer Method Description	8
2.4.2 Morgenstern and Price's Method Description	9
2.5 Numerical Method and Shear Strength Reduction (SSR) Technique	10
2.6 Factor of Safety (FS)	12
2.7 Comparison from Others (Previous) Studies	14
CHAPTER III: 3. LIMIT EQUILIBRIUM AND NUMERICAL METHODOLOGY	16
3.1 GEOSTASE (Limit Equilibrium Based)	16
3.2 FLAC (Numerical Based)	17
3.3 Slope Stability Analysis	18
3.4 The Five Case Studies	19
3.4.1 Case (1): Unreinforced Homogeneous Slope	19
3.4.2 Case (2): Non-Homogeneous Slope with a Thin Weak Layer	20
3.4.3 Case (3): Levee Embankment Slope	22
3.4.4 Case (4): Deep Slope with a Storage Tank	23
3.4.5 Case (5): MSE Wall Modeled with Soil Nails	24

Chapter	Page
CHAPTER IV: 4. RESULTS and DISCUSSIONS	27
4.1 Introduction	27
4.2 Case (1): Unreinforced Homogeneous Slope	27
4.2.1 Analysis Result of Case (1) by GEOSTASE	28
4.2.2 Analysis Result of Case (1) by FLAC	30
4.2.3 Comparison	34
4.3 Case (2): Non-Homogeneous Slope with a Thin Weak Layer	35
4.3.1 Analysis Result of Case (2) by GEOSTASE	35
4.3.2 Analysis Result of Case (2) by FLAC	37
4.3.3 Comparison	41
4.4 Case (3): Levee Embankment Slope	41
4.4.1 Analysis Result of Case (3) by GEOSTASE	42
4.4.2 Analysis Result of Case (3) by FLAC	44
4.4.3 Comparison	48
4.5 Case (4): Deep Slope with a Storage Tank	48
4.5.1 Analysis Result of Case (4) by GEOSTASE	49
4.5.2 Analysis Result of Case (4) by FLAC	51
4.5.3 Comparison	55
4.6 Case (5): MSE Wall Modeled with Soil Nails	56
4.6.1 Analysis Result of Case (5) by GEOSTASE	56
4.6.2 Analysis Result of Case (5) by FLAC	58
4.6.3 Comparison	61
CHAPTER V: 5. SUMMARY AND CONCLUSIONS	62
5.1 Summary	62
5.2 Conclusion	64
5.3 Recommendations	65
REFERENCES	67

LIST OF TABLES

Table	Page
Table 2.1: Recommended minimum values of factor of safety	13
Table 2.2: Factor of safety criteria from U.S. Army Corps of Engineers' slope stability manual	14
Table 3.1: Soil properties in case (1)	20
Table 3.2: Soil properties in case (2)	21
Table 3.3: Soil properties in case (3)	22
Table 3.4: Soil properties in case (4)	24
Table 3.5: Soil properties in case (5)	25
Table 3.6: Reinforcement properties in case (5)	26
Table 4.1: Computed factor of safety from GEOSTASE for case (1)	28
Table 4.2: Computed factor of safety from GEOSTASE for case (2)	35
Table 4.3: Computed factor of safety from GEOSTASE for case (3)	42
Table 4.4: Computed factor of safety from GEOSTASE for case (4)	49
Table 4.5: Computed factor of safety from GEOSTASE for case (5)	56
Table 5.1: Factor of safety results for all cases and failure surface observation	63

LIST OF FIGURES

Figure	Page
Figure 2.1: Different slope failure modes	6
Figure 2.2: Coordinates for noncircular slip surface used in Spencer's procedure. ..	9
Figure 3.1: Geometry and boundary condition of case (1)	20
Figure 3.2: Geometry and boundary condition of case (2)	21
Figure 3.3: Geometry and boundary condition of case (3)	23
Figure 3.4: Geometry and boundary condition of case (4)	24
Figure 3.5: Geometry and boundary condition of case (5)	26
Figure 4.1: Profile preview from GEOSTASE for case (1).....	29
Figure 4.2: Plot of all failure of surfaces from GEOSTASE for case (1).....	29
Figure 4.3: Plot of critical failure surfaces from GEOSTASE for case (1)	30
Figure 4.4: Shear strain plot and FS from FLAC for case (1)	31
Figure 4.5: Mesh plot shows stress and strain quadrilateral element from FLAC for case (1)	31
Figure 4.6: Contour plot for total stresses zones from FLAC for case (1)	32
Figure 4.7: Contour plot for effective stresses zones from FLAC for case (1)	32
Figure 4.8: Contour plot for pore water pressure zones from FLAC for case (1) ...	33
Figure 4.9: Displacement direction plot from FLAC for case (1)	33
Figure 4.10: Critical surface from LEM depicted on shear strain from FDM for case (1)	34
Figure 4.11: Profile preview from GEOSTASE for case (2).....	36
Figure 4.12: Plot of all failure of surfaces from GEOSTASE for case (2).....	36
Figure 4.13: Plot of critical failure surfaces from GEOSTASE for case (2)	37
Figure 4.14: Shear strain plot and FS from FLAC for case (2)	38
Figure 4.15: Mesh plot shows stress and strain quadrilateral element from FLAC for case (2)	38
Figure 4.16: Contour plot for total stresses zones from FLAC for case (2)	39
Figure 4.17: Contour plot for effective stresses zones from FLAC for case (2)	39
Figure 4.18: Contour plot for pore water pressure zones from FLAC for case (2) ..	40
Figure 4.19: Displacement direction plot from FLAC for case (2)	40
Figure 4.20: Critical surface from LEM depicted on shear strain from FDM for case (2)	41

Figure 4.21: Profile preview from GEOSTASE for case (3).....	43
Figure 4.22: Plot of all failure of surfaces from GEOSTASE for case (3).....	43
Figure 4.23: Plot of critical failure surfaces from GEOSTASE for case (3).....	44
Figure 4.24: Shear strain plot and FS from FLAC for case (3)	45
Figure 4.25: Mesh plot shows stress and strain quadrilateral element from FLAC for case (3)	45
Figure 4.26: Contour plot for total stresses zones from FLAC for case (3)	46
Figure 4.27: Contour plot for effective stresses zones from FLAC for case (3)	46
Figure 4.28: Contour plot for pore water pressure zones from FLAC for case (3)	47
Figure 4.29: Displacement direction plot from FLAC for case (3)	47
Figure 4.30: Critical surface from LEM depicted on shear strain from FDM for case (3)	48
Figure 4.31: Profile preview from GEOSTASE for case (4).....	50
Figure 4.32: Plot of all failure of surfaces from GEOSTASE for case (4).....	50
Figure 4.33: Plot of critical failure surfaces from GEOSTASE for case (4)	51
Figure 4.34: Shear strain plot and FS from FLAC for case (4)	52
Figure 4.35: Mesh plot shows stress and strain quadrilateral element from FLAC for case (4)	52
Figure 4.36: Contour plot for total stresses zones from FLAC for case (4)	53
Figure 4.37: Contour plot for effective stresses zones from FLAC for case (4)	53
Figure 4.38: Contour plot for pore water pressure zones from FLAC for case (4)	54
Figure 4.39: Displacement direction plot from FLAC for case (4)	54
Figure 4.40: Critical surface from LEM depicted on shear strain from FDM for case (4)	55
Figure 4.41: Profile preview from GEOSTASE for case (5).....	57
Figure 4.42: Plot of all failure of surfaces from GEOSTASE for case (5).....	57
Figure 4.43: Plot of critical failure surfaces from GEOSTASE for case (5).....	58
Figure 4.44: Shear strain plot and FS from FLAC for case (5)	59
Figure 4.45: Mesh plot shows stress and strain quadrilateral element from FLAC for case (5)	59
Figure 4.46: Contour plot for total stresses zones from FLAC for case (5)	60
Figure 4.47: Displacement direction plot from FLAC for case (5)	60
Figure 4.48: Critical surface from LEM depicted on shear strain from FDM for case (5)	61

CHAPTER I

1. INTRODUCTION

1.1 Background

Slope stability analysis is an important and delicate problem in civil engineering, particularly for large projects such as dams, mining, highways and tunnels. Many techniques exist for evaluation of the stability of a given slope. The main interest of slope stability analysis is typically to determine a factor of safety value (FS) against slope failure. A lot of researches have been performed in the last the past few decades but slope stability analysis still remains a challenge in geotechnical engineering.

Many alternative slope stability analysis methods have been proposed. In general, these slope stability analysis methods fall into two categories: the limit equilibrium method (LEM) and the numerical method have been widely used.

The limit equilibrium analysis is based on determining applied forces and mobilized strength over a trial slide surface in the soil slope. Generally, different LEM typically divide soil mass into many slices and assume different interslice normal and shear forces in order to achieve a statically determine solution.

Lately, attention has been paid to the slope stability evaluations using finite element (FEM) or finite difference method (FDM). The FEM or FDM can capture the soil stress-strain behavior and thus eliminate the assumptions needed in LE methods to bring the static-indeterminate problem to a statically determinate one. The Shear Strength Reduction (SSR) technique has been implemented to calculate FS for FDM.

Generally, LEM is based on assumptions on interslice forces. In contrast, SSR method does not have divided slices as in LEM. However, SSR and LEM methods do share one thing in common: there is only one constant factor of safety along the potential slip surface (Griffiths and Lane, 1999). In previous studies, much research had been done on generated simple cases and conducted with one method. The use of two different methods may give different results but the synergism of both methods can give valuable source of check on the slope failure mechanism. This thesis presents real cases of studies, rather than simple generated cases, that involves different real situations of geometry and soil profiles using Spencer, Morgenstern and Price's, and SSR methods.

1.2 Objective

Limit equilibrium and numerical methods may give different results on the same slope. Comparisons of the two methods have been made by other researchers, but mostly with simplified slopes. The objective of this research is to study the difference of the factor of safety by both limit equilibrium and numerical methods for a five real cases.

1.3 Methodology

In this study, five different types of real slopes with complex geometry and external influences were analyzed by both limit equilibrium and finite difference methods to gain more insight for a relevant factor of safety and the slip surface. Two slope stabilities software were used in this research: GEOSTASE[®] based on LEM and FLAC[®] based on FDM.

The five cases of the stability analysis are:

- (1). An Unreinforced Homogeneous Slope
- (2). A Non-Homogeneous Slope with a Thin Weak Layer
- (3). A Levee Embankment Slope
- (4). A Deep Slope with a Storage Tank
- (5). A MSE Wall Modeled with Soil Nails

1.4 Organization of the Thesis

This thesis contains five chapters. The first chapter introduces the overall background, factor of safety, the objective, and methodology of this research. The second chapter is a literature review which examines the theory and previous studies related to this area. The third chapter describes the software and the five slope cases used in this research. The forth chapter provides the slope stability analysis and results obtained from the two software. Finally, the last chapter presents the conclusions and recommendations from this research.

CHAPTER II

2. LITERATURE REVIEW

2.1 Introduction

A wide range of slope stability analyses are performed using general-purpose computer programs. There are many options and features to be considered such as soil strength, pore water pressure, reinforcement, slip surfaces, and procedure of analysis. Each of these options and features have sub combinations that lead to about thousands probable options and features for a comprehensive slope stability computer program. Obviously, it is not possible to test sophisticated computer programs for every possible combinations of data, or even a reasonably small fraction of the possible combinations (Duncan and Wright, 2005).

Consequently, there is a high possibility that many computer programs have not been tested for the exact combination. Moreover, using simple equations can lead to approximations that can cause, in some cases, significant errors. Also, it is possible to make errors in input data due to different program assumption and from human errors. Therefore, independent checks should be made regardless of how slope stability computations are performed.

2.2 Types of Slope Failures and Instability Mechanism

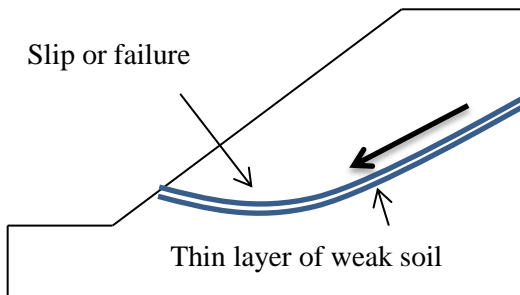
There are many conditions that affect slope failures depending on the soil type, soil stratification, ground water, seepage, and the slope geometry (Budhu, 2000).

Failure of a slope along a weak zone of soil is called a translational slide Figure 2.1(a). In coarse-grained soils, translational slides are common. In this case, the sliding mass can travel long distances before coming to rest

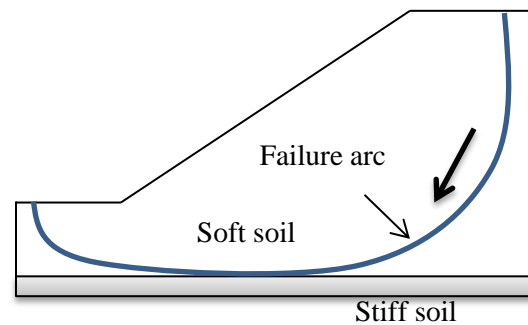
A common type of failure in homogeneous fine-grained soils is a rotational slide that has its point of rotation on an imaginary axis parallel to the slope (Duncan, 2005).

Brief descriptions of three types of rotational failure that often occur are given below:

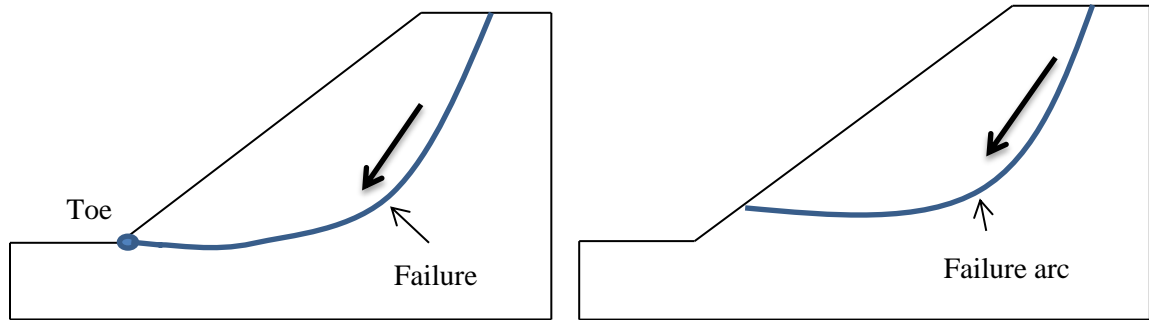
- Base slide: occurs by an arc engulfing the whole slope. A soft soil layer resting on a stiff layer of soil is prone to base failure and passes below the toe Figure 2.1(b).
- Toe slide: whereby the failure surface passes through the toe of the slope Figure 2.1(c).
- Slope slide: whereby the failure surface passes through the slope and above the toe Figure 2.1(d).



(a): Movement of soil mass along a thin layer of weak soil



(b): Base slide



(c): Toe slide

(d): Slope slide.

Figure 2.1 Different slope failure modes (Duncan, 2005; Chen, 1995; Budhu, 2000).

For purpose of designing, constructing, repairing failed and damaged slopes, it is important to understand the causes of instability in slopes.

In most cases, several causes exist simultaneously. For example, water influences affect the slope in many ways, making impossible to isolate one effect. Moreover the behavior of clay soils is complex and unpredictable whether from softening, progressive failure, or a combination. According to Sowers (1979), it is usually not possible to identify the cause that acted alone and resulted in instability, and it is also incorrect technically to isolate one cause.

Attempting to identify which one finally produced the failure is not only difficult, but also technically inaccurate (Duncan and Wright, 2005). Therefore, in designing and constructing new slopes, it is important to consider potential changes in properties and conditions that may affect the structure during its life so that it will remain stable despite these changes.

To prevent slope failure, the shear strength of the soil must be greater than the shear stress requirement for equilibrium. The instability condition can be obtained through two mechanisms (Duncan and Wright, 2005):

The first mechanism a decrease in the shear strength, the maximum shear stress that the soil can withstand, may occur due to an increase in void ratio (swelling), increase in moisture content, increase in pore water pressure, development of slickenside, creep under sustained loads, and weathering. The second mechanism an increase in the shear stress may occur due to water pressure causing saturation of soils, drop in water level, load at the top of the slope, and earthquake.

2.3 Shear Failure and Mohr-Coulomb Model Description

A shear failure in which movement caused by shearing stresses in a soil mass sufficient magnitude to move a large slope mass or a slope with its foundation relative to the adjacent stationary mass. A shear failure is most likely to occur along a discrete surface as assumed in stability analyses, although the shear movements may in fact occur across a zone of appreciable thickness.

Failure of a soil element at a certain location does not mean failure of the system. However there is no single cause of failure. It could mean a reduction in the resistance and as a result a reduction to the factor of safety.

The Mohr-Coulomb failure criterion is the most commonly used one in soil mechanics. The Mohr-Coulomb equation can be written as a function of normal stress (σ) and shear stress (τ) on the failure plane:

$$\tau_f = c' + \sigma'_f \tan \phi' \dots \dots \dots (2.1)$$

where τ_f is shear strength at failure, c' is effective cohesion, σ'_f is effective stress at failure, and ϕ' is the effective angle of friction.

2.4 Limit Equilibrium Method

The shear strength of the soil is reduced by a significant factor of safety to reach the equilibrium against the shear stresses. This calculation is called limit equilibrium procedure (Duncan and Wright, 2005).

There are two approaches for satisfying static equilibrium. The first approach is to consider the equilibrium for the entire mass of soil and solved for a single free body. The other approach is to divide the soil into a number of slices and each slice has to satisfy all forces to equilibrium (Duncan and Wright, 2005).

Several different procedures of slices satisfy static equilibrium completely. Each of these procedures makes different assumptions to achieve a statically determinate solution. In this study, the slice approach for Spencer's procedure and Morgenstern and Price's procedure were used which satisfy all the requirements for static equilibrium. Regardless of whether equilibrium is considered for a single free body or a series of individual vertical slices, there are more unknowns (forces, locations of forces, factor of safety, etc.) than the number of equilibrium equations; the problem of computing a factor of safety is statically indeterminate. Therefore, assumptions must be made to achieve a balance of equations and unknowns.

2.4.1 Spencer's Method Description

In 1967, Spencer developed a complete equilibrium method known as Spencer's method, which satisfies both force and moment equilibrium. Spencer's Method used for circular slip surface and can also be adapted for use with non-circular slip surface (see Figure 2.1), which is useful because many slides do not have circular failure surface (Spencer, 1967).

Spencer's procedure is based on the assumption that the interslice forces are parallel and have the same inclination. The inclination is unknown and is computed as one of the unknowns in solution of the equilibrium equations. The other assumption is that the normal force acts at the center of the base of each slice. However, this assumption has negligible influence on the computed values for the unknowns provided that a reasonably large number of slices are used (Duncan and Wright, 2005).

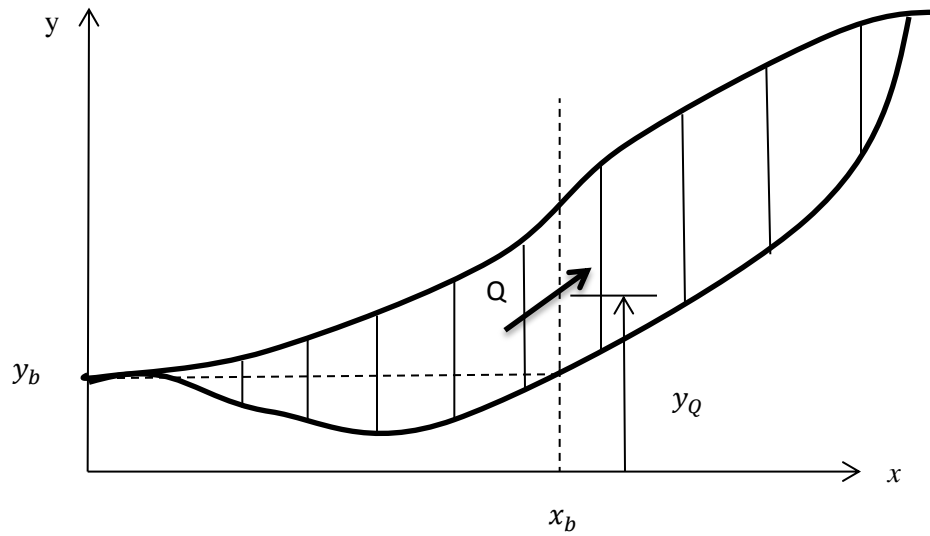


Figure 2.2 Coordinates for noncircular slip surface used in Spencer's procedure.

2.4.2 Morgenstern and Price's Method Description

Morgenstern and Price's (1965) procedure is similar to Spencer's procedure. The only major difference between Morgenstern and Price's and Spencer's procedures in terms of unknowns is that Spencer's procedure involves a single interslice shear force inclination whereas Morgenstern and Price's procedure involves different interslice shear force inclination that function on x direction (Duncan and Wright, 2005).

2.5 Numerical Method and Shear Strength Reduction (SSR) Technique

The numerical is a powerful tool for solving many engineering problems. With recent advancements in computer technology, the finite difference or element method has become more and more popular in geotechnical engineering analysis. Two of the most commonly used numerical methods are the finite element method (FEM) and finite difference method (FDM).

The shear strength reduction technique is a computed procedure to determine the factor of safety of slope by reducing the shear strength of the soil until failure occurs. It is a relatively new technique and has become more popular than before due to increasing speed of desktop computer. It was originally proposed by Zienkiewicz in 1975. The maximum nodal force vector is also called the unbalanced or out-of-balance force. The maximum unbalanced force will never exactly reach zero for a numerical analysis. The model is considered to be in equilibrium when the maximum unbalanced force is small compared to the total applied forces in the problem. If the unbalanced force approaches a constant nonzero value, this probably indicates that failure and plastic flow are occurring within the model. The ratio of the soil's actual shear strength to the reduced shear strength to failure is the factor of safety. In SSR finite element and finite difference technique assumed, the slope material behavior are plastic-elastic. However, there has been little investigation in the accuracy of this technique. Importantly, in this technique the critical failure surface is found automatically compare to the LEM (Dawson et al, 1999).

The Shear Strength Reduction (SSR) technique (Dawson et al, 1999, Griffith and Lane, 1999, Hammah et al, 2004) enables the FEM to calculate factors of safety for slopes. The method enjoys several advantages including the ability to predict stresses and deformations of support elements, such as piles, anchors, and geotextiles at failure. The technique makes it possible to visualize the development of failure mechanisms.

In this technique from Mohr-Coulomb strength parameters the modification is as follows (Hammah, 2005):

$$C'_{trial} = \frac{1}{FS_{trial}} C'_{measured} \dots \dots (2.2)$$

$$\phi'_{trial} = \tan^{-1} \left(\frac{1}{FS_{trial}} \tan \phi \right) \dots \dots \dots (2.3)$$

$$\tau_{max} = C'^{(i)}_{trial} + \sigma_n \tan \phi'^{(i)}_{trial} \text{ for the } i^{th} \text{ material } \dots \dots (2.4)$$

where, for SSR analyses, the same “strength reduction factor” ($SSR = FS_{trial}$) is used for all components of strength and all materials within the stability problem (Diederichs et al., 2007).

For Mohr-Coulomb materials, the steps for systematically searching for the critical factor of safety value, FS, which bring a previously stable slope to the verge of failure, are given below by Rocscience (2004):

“Step 1: Develop an FE model of a slope, using the deformation and strength properties established for the slope materials. Compute and record the maximum total deformation in the slope by the finite element method.

Step 2: Increase the value of FS and calculate factored Mohr-Coulomb material parameters as described above. Enter the new strength properties into the slope model and re-compute deformation. Record the maximum total deformation.

Step 3: Repeat Step 2, using systematic increments of FS, until the FE model does not converge to a solution. In other words, continue to reduce material strength until the slope fails. The critical FS value beyond which failure occurs will be the slope factor of safety, based on the finite element method.

For a slope that is initially unstable, factor of safety values in steps 2 and 3 must be reduced until the finite element model converges to a solution. Similarly, these steps can be done on FDM (Rocscience, 2004).”

2.6 Factor of Safety (FS)

The factor of safety (FS) is the primary design criteria used in the slope stability analysis. Traditional limit equilibrium based methods are still widely used in practice while at the same time the finite element or finite difference based are different source of evaluating of slope stability. The Shear Strength Reduction technique is one of the popular methods to compute the FS utilizing finite difference and finite element analysis.

The most basic purpose of slope stability analysis is to determine a factor of safety against a potential failure, or landslide. If this factor of safety is determined to be large enough, the slope is judged to be stable (safe). If it is 1.0 or less, it is unsafe. In this research, we study and discuss Limit Equilibrium and Numerical Methods results from different cases.

The main assumption of the factor of safety in limit equilibrium is that the factor of safety is the same at all points along the slip surface. Therefore, the value represents an average or overall value for the assumed slip surface. If failure were to occur, the shear stress would be equal to the shear strength at all points along the failure surface and the assumption that the factor of safety is constant would be valid. If, instead, the slope is stable, the factor of safety probably varies along the slip surface (e.g., Wright et al., 1973). However, this should not be of significant consequence as long as the overall the factor of safety is suitably greater than 1.0 and the assumed shear strengths can be fully mobilized along the entire slip surface (Duncan and Wright, 2005).

To have a boundary between stability and instability of the slope, a value of $FS = 1.0$ indicates that stable which means the shear strength of soil equals the shear stress. If all the factors are computed precisely, a value of 1.1 or even 1.01 would be acceptable. However, because the quantities involved in computed values of the FS are not precise, due to uncertainty of variables, thus, the factor of safety should be larger to insure the safety of the slope from failure (Duncan and Wright, 2005).

The uncertainty regarding analysis conditions should be considered with a value of factor of safety. Recommended minimum values of factor of safety are shown in Table 2.1 (Duncan and Wright, 2005).

Table 2.1: Recommended minimum values of factor of safety (Duncan and Wright 2005)

Cost and consequences of slope failure	Uncertainty of analysis conditions	
	Small	Large
Cost of repair comparable to incremental cost to more conservatively designed slope	1.25	1.5
Cost of repair much greater than incremental cost to construct more conservatively designed slope	1.5	2.0 or greater

Based on experience, U.S. Army Corps of Engineers developed a factor of safety Criteria of slope Stability Manual presented in Table 2.2

Table 2.2: Factor of safety criteria from U.S. Army Corps of Engineers' slope stability manual

Types of Slopes	Required factors of safety		
	For end of construction	For long-term steady seepage	For rapid drawdown
Cost of repair comparable to incremental cost to more conservatively designed slope	1.3	1.5	1.0-1.2

Another approach of factor of safety of slopes refers to the ratio of resisting moment to overturning moment on circular slip surfaces (Duncan, 2005).

2.7 Comparison from Other (Previous) Studies

Cheng et al. (2006) performed slope stability analysis by limit equilibrium method and strength reduction method on several simplified slopes cases. This study compared the limit equilibrium results with shear strength reduction method of slope stability analysis. The slope stability examples were performed on homogenous and nonhomogeneous slopes with various material properties. It was found that for homogenous slopes the result are generally in good agreement. They concluded that both the LEM and SSR have their own merits and limitations, and the use of the SSR is not really superior to the use of the LEM in routine analysis and design. Both methods should be viewed as providing an estimation of the factor of safety and the probable failure mechanism, but engineers should also appreciate the limitations of each method when assessing the results of their analyses.

In another study (Hammah et al, 2004), a finite element analysis of a soil slope through SSR technique was performed. They compare the method's performance to the most widely used limit equilibrium on large range of slope cases. The SSR's performance tested on about 30

generated slope examples and used by software developers to verify the results of traditional slope stability programs. The results showed that in almost all of these unreinforced slope cases, the number of elements had little impact on SSR factor of safety. The author recommends adopting the SSR as an additional robust and powerful tool for design and analysis. However, the author recommended further research to be conducted.

Wei et al. (2010) presented a case study that using Spencer's method, SSR, and directly finite element computed normal and shear stresses to evaluate the slope stability factor of safety. It was found that the method that directly used the finite element computed stresses can capture the relatively deep slip surface well. Also, conventional LEM cannot take the initial stress state into account; the slice forces are determined by static equilibrium which may not be realistic. However, it was recommended by the authors that a conventional method, such as Spencer method, be applied to identify the possible location of the "imaginary" slip surface. Moreover, it seemed that the SSR method, with a reasonable lateral earth pressure coefficient value to establish the initial stress state, tends to yield a higher factor of safety than Spencer or FES method.

Griffiths and Lane (1999) described six generated simplified slope examples of finite element slope stability analysis with a comparison against other traditional limit equilibrium methods, including the influence of layering and free surface on slope and dam stability. It was concluded the numerical method was a powerful alternative to traditional limit equilibrium methods and its widespread use should now be standardized in geotechnical practice.

CHAPTER III

3. LIMIT EQUILIBRIUM AND NUMERICAL METHODOLOGY

3.1 GEOSTASE[®] (Limit Equilibrium Method Based)

GEOSTASE[®] is a 2-D limit equilibrium slope stability analysis software program written by Dr. Garry H. Gregory. The name GEOSTASE is an acronym for General Equilibrium Options for Stability Analyses of Slopes and Embankments. The name is a United States Registered Trademark owned by Dr. Gregory. The program was written in Visual Fortran for the Microsoft Windows[®] operating system and explicitly accommodates either English or SI units.

GEOSTASE contains options for analysis of slope stability using a variety of popular limit equilibrium methods including the Spencer Method, Morgenstern-Price Method, Simplified Bishop Method, Simplified Janbu Method, United States Army Corps of Engineers (USACE) Modified Swedish Method, and the Lowe and Karafiath Method. The Spencer and Morgenstern-Price methods satisfy both force and moment equilibrium. The Simplified Bishop Method satisfies moment equilibrium and vertical force equilibrium, but not horizontal force equilibrium, and the remaining methods satisfy only force equilibrium. The Spencer and Morgenstern-Price methods were used for this study.

GHOSTASE provides explicit options for reinforcing elements and external loads including piers/piles, tiebacks (anchors), soil nails, planar reinforcement (geogrids), applied forces, a generic reinforcement option, boundary (surcharge) loads, earthquake (seismic) loads, water surfaces and loads, and tension cracks. Search options are provided for generating an essentially unlimited number of trial failure surfaces including circular, block, and non-circular surfaces. Individual failure surfaces can also be included for any shape surface. Soil options include basic (isotropic) soil parameters, anisotropic soil parameters, non-linear undrained shear strength variation with depth and/or horizontal position, curved strength envelope, and fiber-reinforced soil. Portions of the geometry (such as hard rock) can be excluded from the search areas (if desired) by the use of “Xclude” lines in the profile.

GHOSTASE includes an interactive user-friendly interface and high-quality graphics and text output. Many of the features and options in the program were used in the analysis of the five case study slopes in this study.

3.2 FLAC[®] (Numerical Analysis Method Based)

FLAC[®] is a 2-D limit equilibrium finite difference analysis program developed by Itasca Consultant Group Inc. The name FLAC is an acronym for **F**ast **L**agrangian **A**nalysis of **C**ontinua. FLAC is specially designed for geotechnical and geological engineering computations. The program has 14 built-in constitutive models to simulate the behavior of geotechnical structures built of soil, rock, and other construction materials. FLAC also provides explicit options for reinforcing elements and external loads including piers/piles, tiebacks (anchors), soil nails, planar reinforcement (geogrids), applied forces, a generic reinforcement option, boundary (surcharge) loads, earthquake (seismic) loads, water surfaces and loads, and tension cracks.

In this study, the soil is considered as a linear-elastic perfect-plastic material with a Mohr-Coulomb yield criterion.

3.3 Slope Stability Analysis

The five real cases were analyzed by both methods to study the effects on the slope factor of safety. The results from the numerical method were compared with conventional methods. The first case was analyzed for a condition of an unreinforced homogenous slope. The second and the third cases analyzed a non-homogeneous slope with different water levels. Also the forth case was analyzing the influence of existing structure in a non-homogeneous slope. The last case was analyzed to better understand the stability improvements using reinforced strips modeled as soil nails, and their influence on failure plane and the factor of safety form both methods.

The conventional methods (limit equilibrium) were used based on Spencer and Morgenstern and Price's methods. There are many methods such as Bishop's Simplified Method (1955), the Modified Swedish Method and Janbu Method (1968). In this study were used Morgenstern and Price's Method (Morgenstern and Price, 1965), and Spencer's Method (Spencer, 1967). These methods generally differ from one to another in the equations of static equilibrium and the relationship between the interslice and the shear forces (Shiu et al., 2006). A difficulty with all the conventional methods is that they are based on an assumption and that assumption is based on the shape or the location of surface of failure (Griffiths and Lane, 1999). Additionally, critical slip surface of failure at the minimum factor of safety from LEM was observed and depicted on shear strain increment path from FDM.

The finite difference method and limit equilibrium based on a non-associative Mohr-Coulomb plasticity were used in all cases throughout this paper. Numerical analysis was

performed to investigate states of failure and investigate the location of the slip surface due to strength parameters and existing conditions.

The computer software package General Equilibrium Options for Stability Analysis of Slopes and Embankment GEOSTASE[®] (General Equilibrium Options for Stability Analysis of Slopes and Embankments) developed by Gregory Geotechnical was used to determine of the factor of safety values obtained from the limit equilibrium methods. Also another software package FLAC[®] (Fast Lagrangian Analysis of Continua) developed by Itasca Consulting Group Inc. was used to obtain the factor of safety via numerical method as mentioned above.

3.4 The Five Cases of Studies

Five slope cases were evaluated in this study : (1) an unreinforced homogeneous slope, (2). a non- homogeneous slope with a thin weak layer, (3) a levee embankment slope, (4) a deep slope with a storage tank and (5) a MSE wall modeled with soil nails.

3.4.1 Case (1): Unreinforced Homogenous Slope

This project consisted of a non-reinforced homogeneous slope which was an embankment for a commercial shopping center development. The slope was constructed against an existing natural slope with a water table. The slope was constructed in Virginia many years ago and has not experienced any failures since construction.

The soils' properties of case (1) are shown in Table 3.1. The dimensions and boundary conditions are shown in Figure 3.1.

Table 3.1: Soil properties in case (1)

Soil Number	Soil Description	Moist Unit Weight (pcf)	Saturated Unit Weight (pcf)	Cohesion (psf)	Friction angle (degree)
1	Sandy Clay	120	120	300	30
2	Firm Soil	130	130	500	35

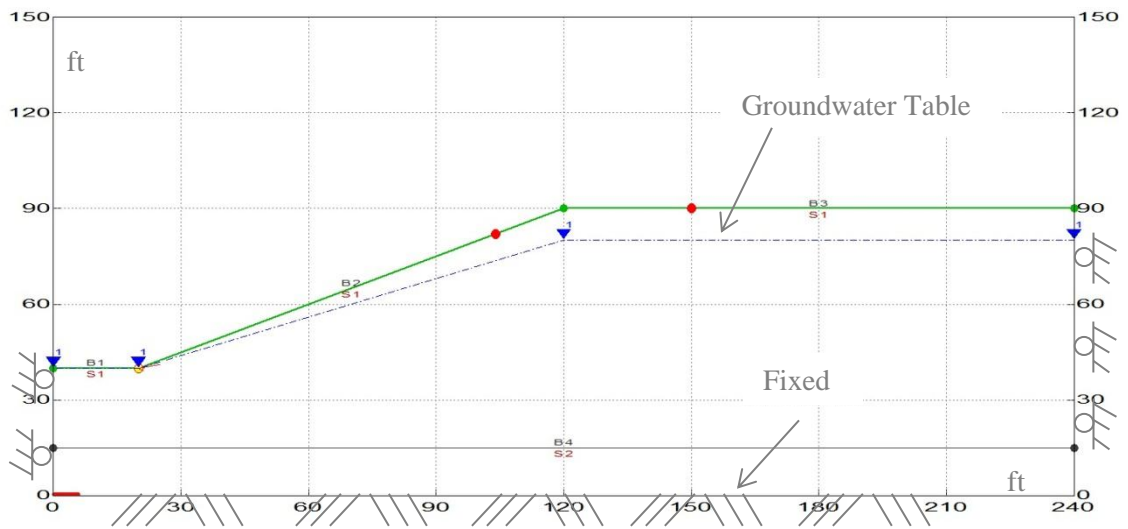


Figure 3.1: Geometry and boundary condition of case (1)

3.4.2 Case (2): Non-Homogenous Slope with a Thin Weak Layer

This slope is an embankment slope on a major arterial roadway in Grand Prairie, Texas. A seismic coefficient was required for the project and specified with horizontal earthquake coefficient (K_h) = 0.03 g. This slope was experiencing a creep type failure where the slope was slowly moving toward the adjacent lake and was causing damage to the roadway and light poles.

The soils' properties of case (2) are shown in Table 3.2. The dimensions and boundary conditions are shown in Figure 3.2. The surcharge load stress of 250 psf is applied uniformly within specified horizontal range.

Table 3.2: Soil properties in case (2)

Soil Number	Soil Description	Moist Unit Weight (pcf)	Saturated Unit Weight (pcf)	Cohesion (psf)	Friction angle (degree)
1	Fill-CH-1	120	132	70	16
2	Bentonite Seam1	120	132	0	11
3	Soil cement	130	135	1000	40
4	FRS Fill	120	132	72	12.7
5	Shale	132	140	575	22
6	Fill-CH-2	120	132	500	16

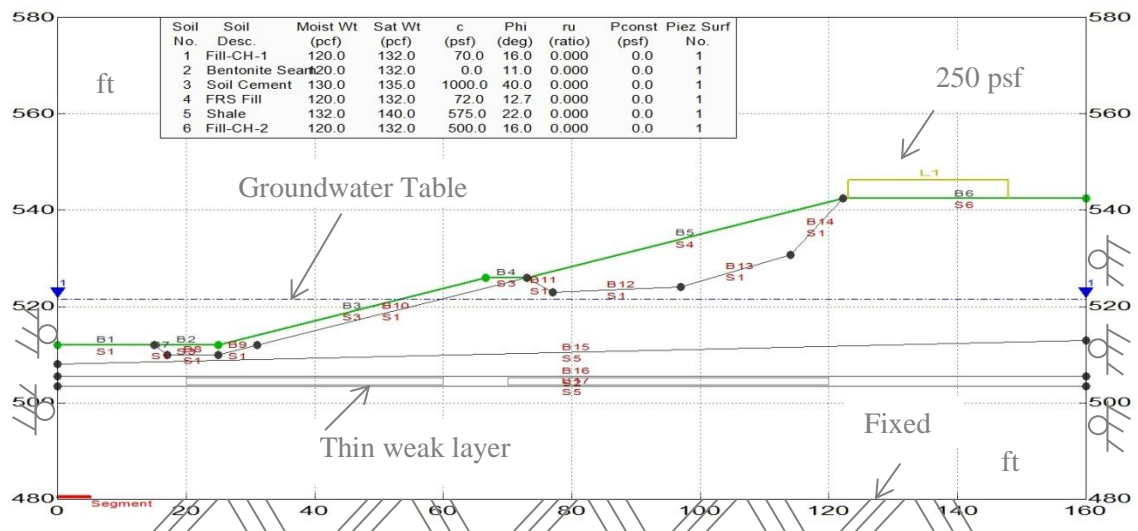


Figure 3.2: Geometry and boundary condition of case (2)

3.4.3 Case (3): Levee Embankment Slope

This slope consists of a lagoon levee for backwash ponds for a water treatment plant in Weatherford, Texas. A seismic coefficient was required for the project and specified with horizontal earthquake coefficient (K_h) = 0.03 g. The lagoon levee was completed in 1998 and no slope failures have occurred.

The soils' properties of case (3) are shown in Table 3.3. The dimensions and boundary conditions are shown in Figure 3.3. The surcharge load stress of 250 psf is applied uniformly within specified horizontal range.

Table 3.3: Soil properties in case (3)

Soil Number	Soil Description	Moist Unit Weight (pcf)	Saturated Unit Weight (pcf)	Cohesion (psf)	Friction angle (degree)
1	Shell	127	132	144	27
2	Core	122	127	200	18
3	Strat A	130	135	225	16
4	Strat B	130	135	285	14

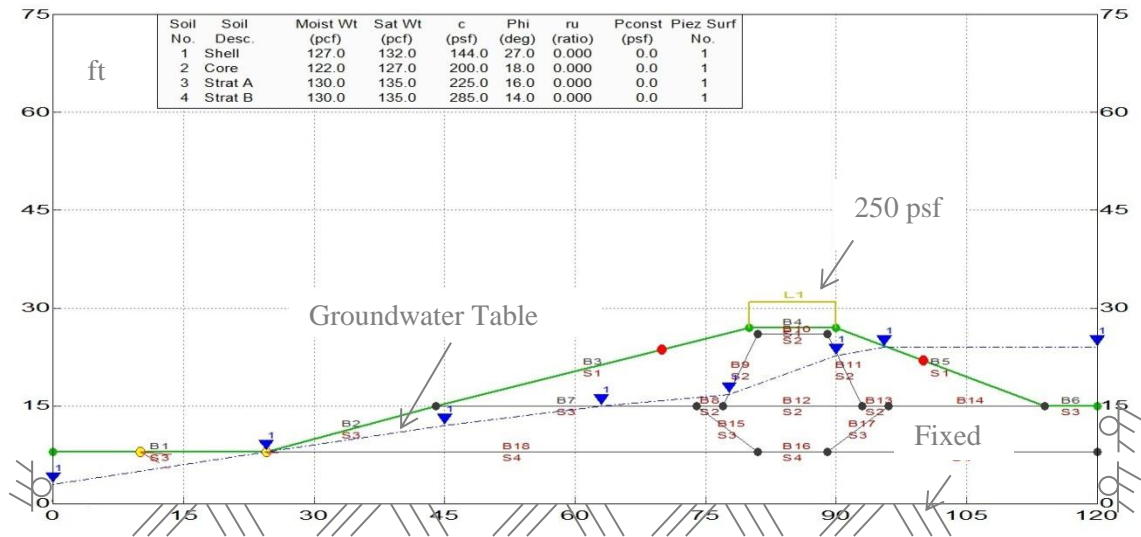


Figure 3.3: Geometry and boundary condition of case (3)

3.4.4 Case (4): Deep Slope with a Storage Tank

This slope was adjacent to a chemical storage tank for a water treatment plant in Parker County, Texas. The slope was experiencing a failure and was endangering the chemical tank. The case modeled in this study was for the initial failure with FS slightly above 1.0. The slope was repaired in 1997 with a large earth berm at the toe and no further failures have occurred.

The soils' properties of case (4) are shown in Table 3.4. The dimensions and boundary conditions are shown in Figure 3.4. The tank is modeled as surcharge load stress of 1800 psf applied uniformly within specified horizontal and vertical range.

Table 3.4: Soil properties in case (4)

Soil Number	Soil Description	Moist Unit Weight (pcf)	Saturated Unit Weight (pcf)	Cohesion (psf)	Friction angle (degree)
1	Fill	125	125	200	28
2	Crib Wall	115	115	0	38
3	SC-CL	128	128	180	26
4	Weak Layer	125	125	0	15
5	Sandstone	135	135	1000	38

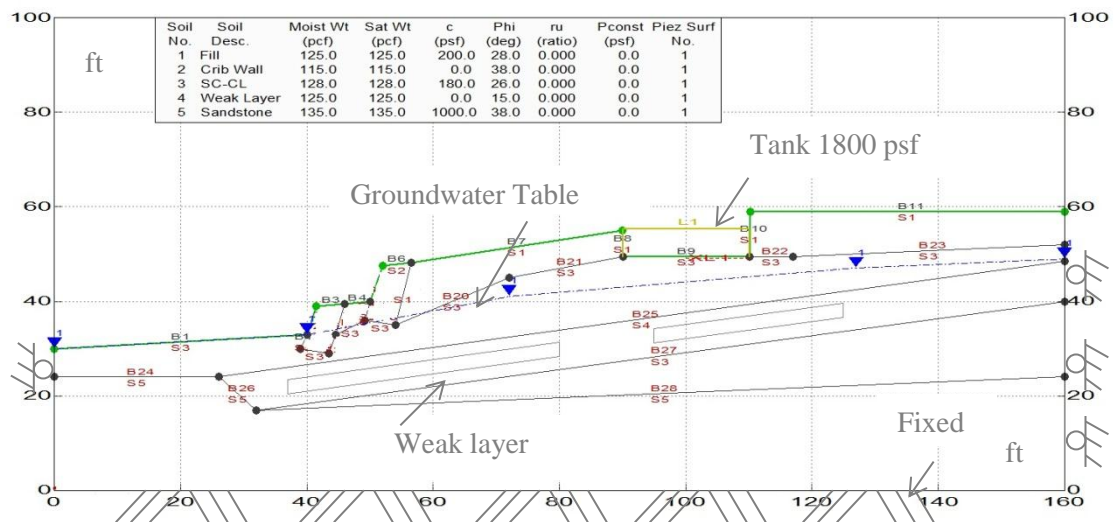


Figure 3.4: Geometry and boundary condition of case (4)

3.4.5 Case (5): MSE wall Modeled with Soil Nails

This slope was in conjunction with an MSE wall on a major state highway in central Texas. The wall was required to make room for a new lane in the toe area of the existing roadway

slope. The compound failure mode (passing near the toe of the proposed wall and exiting in the existing roadway at the top of the slope) was the most critical global slope condition. A minimum FS of 1.3 was required for this failure mode. The existing slope excavation was temporarily supported by short soil nails until the MSE wall was constructed. The project was completed in 2009 and has not experienced any problems.

The soils' properties of case (5) are shown in Table 3.5 and reinforcement properties shown in Table 3.6. The dimensions and boundary conditions are shown in Figure 3.5. The surcharge load stress of 250 psf is applied uniformly within specified horizontal range.

Table 3.5: Soil properties in case (5)

Soil Number	Soil Description	Moist Unit Weight (pcf)	Saturated Unit Weight (pcf)	Cohesion (psf)	Friction angle (degree)
1	Clay	125	125	200	23
2	Siltstone	130	130	0	28
3	Limestone	138	138	1170	30
4	Reinf. Fill	125	128	0	34
5	Retain/Found	125	128	0	30
6	Sat Clay	125	128	0	30

Table 3.6: Reinforcement properties in case (5)

Nail No.	X-Position (ft)	Y-Position (ft)	Nail Dia. (in)	Tendon Dia. (in)	Z-Spacing (ft)	Inclination (degree)	Length (ft)	Young's Modulus, E (psf)
1	60.0	1000.6	1.2	0.5	2.5	0.0	19.0	4.18e9
2	60.0	1003.0	1.2	0.5	2.5	0.0	19.0	4.18e9
3	60.0	1005.5	1.2	0.5	2.5	0.0	19.0	4.18e9
4	60.0	1008.0	1.2	0.5	2.5	0.0	19.0	4.18e9
5	60.0	1010.5	1.2	0.5	2.5	0.0	19.0	4.18e9
6	60.0	1013.0	1.2	0.5	2.5	0.0	19.0	4.18e9
7	60.0	1015.5	1.2	0.5	2.5	0.0	19.0	4.18e9
8	60.0	1018.0	1.2	0.5	2.5	0.0	19.0	4.18e9
9	60.0	1020.5	1.2	0.5	2.5	0.0	19.0	4.18e9
10	60.0	1023.0	1.2	0.5	2.5	0.0	19.0	4.18e9

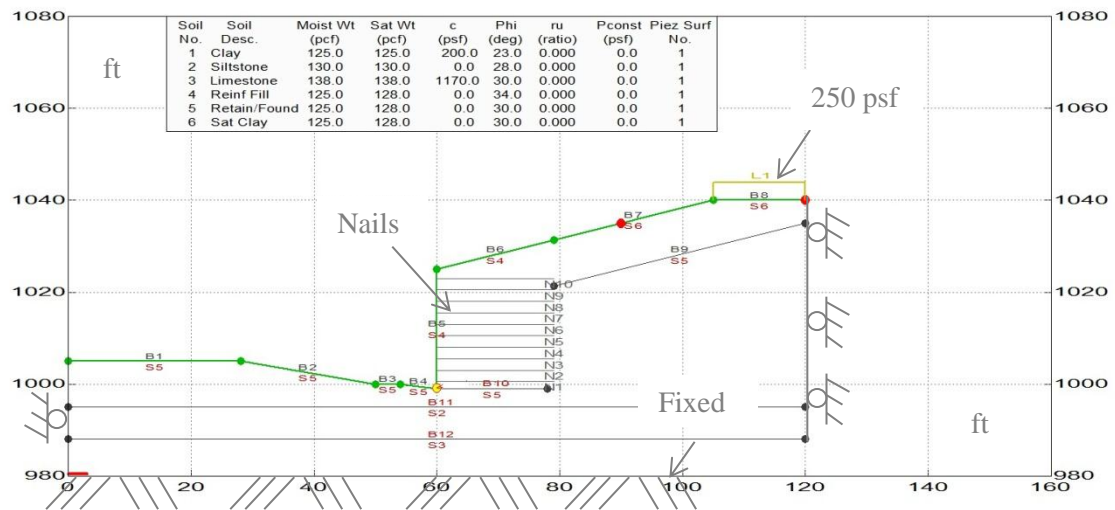


Figure 3.5: Geometry and boundary condition of case (5)

CHAPTER IV

4. RESULTS and DISCUSSIONS

4.1 Introduction

In the present study, limit equilibrium analysis and two-dimensional finite difference analysis were performed using GEOSTASE and FLAC respectively. Both softwares are tools to evaluate the stability of slopes and walls with and without reinforcement. The analyses were performed on five different slopes (geometric models) from five different real projects as described in the previous chapter. The factors of safety for each slope were obtained from both method and were reported in this chapter.

In the limit equilibrium analysis, the factors of safety were obtained by Spencer's and Morgenstern and Price's methods, whereas in the finite difference analysis factors of safety were determined by the Shear Strength Reduction (SSR) technique which was explained in chapters 2.

4.2 Case (1): Results for Unreinforced Homogeneous Slope

The analysis results for both GEOSTASE with limit equilibrium based and FLAC with finite difference based method in this case are shown below.

4.2.1 Analysis Results of Case (1) by GEOSTASE

The Spencer method was used to solve the factor of safety. The geometry of the slope is shown in Figure 4.1. The output calculation of all surfaces of failure is shown in Figure 4.2. The analysis results of the critical surfaces of failure are shown in Figure 4.3. The output results of 10 most critical surfaces of failure are shown in Table 4.1. This is only 10 of most critical surface of failure which selected from total of 1000 surface analyzed. The minimum value of the factor of safety is 1.296 and the circle center coordinate $x = 45.187$ ft and $y = 134.483$ ft with a radius of 97.782 ft.

Table 4.1: Computed factor of safety from GEOSTASE for case (1)

Failure Surface No.	Factor of Safety	Failure Surface Radius (ft)
1	1.296	97.782
2	1.297	96.052
3	1.297	101.382
4	1.297	98.576
5	1.297	102.421
6	1.297	94.348
7	1.298	97.082
8	1.298	103.798
9	1.298	93.806
10	1.299	98.984

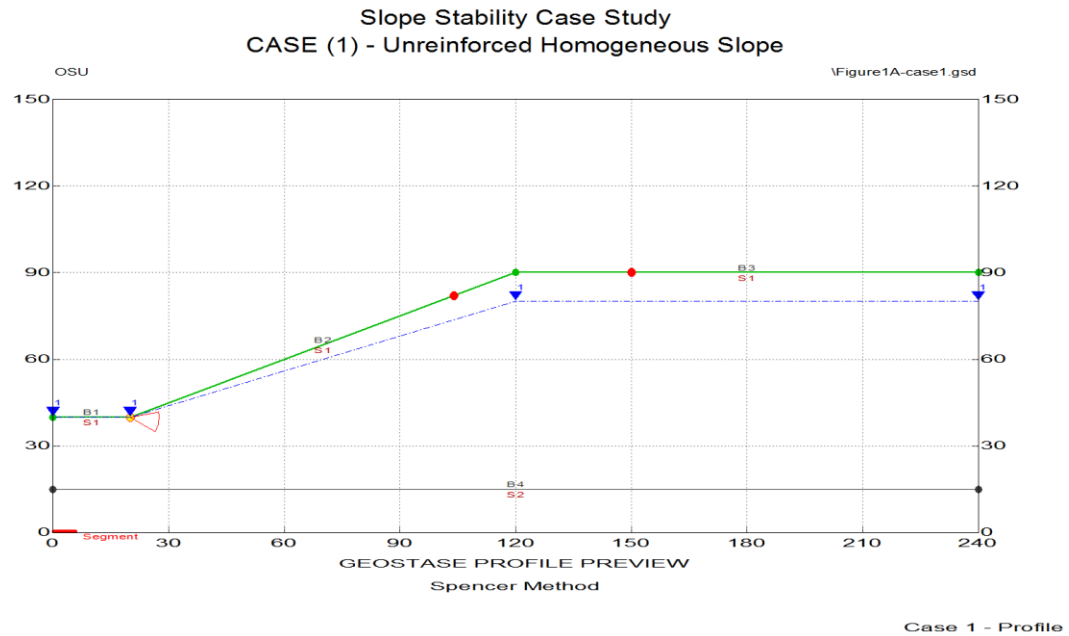


Figure 4.1: Profile preview from GEOSTASE for case (1)

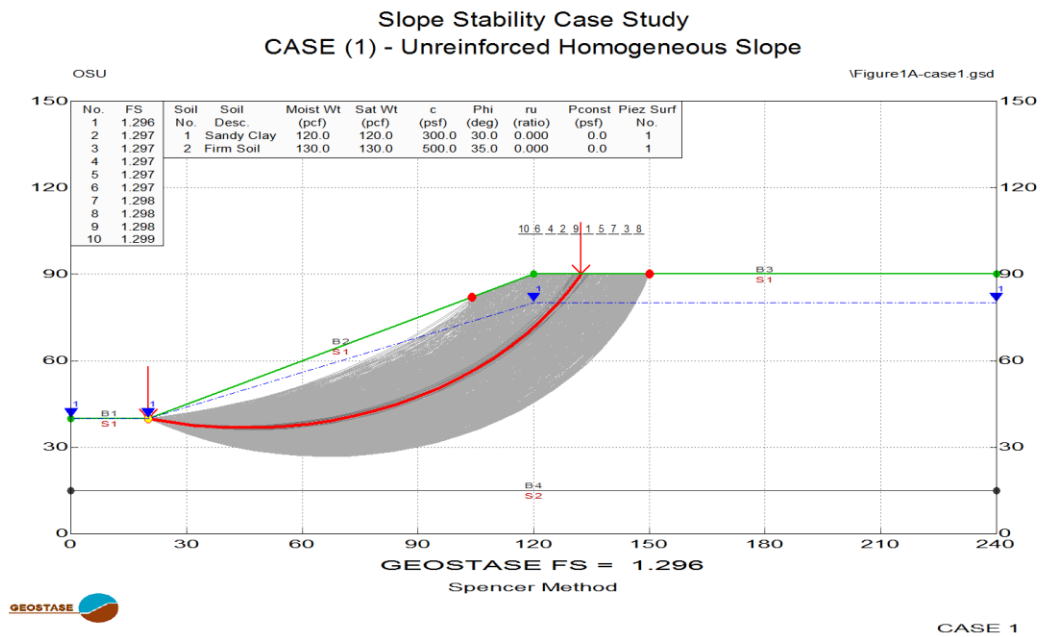


Figure 4.2: Plot of all failure of surfaces from GEOSTASE for case (1)

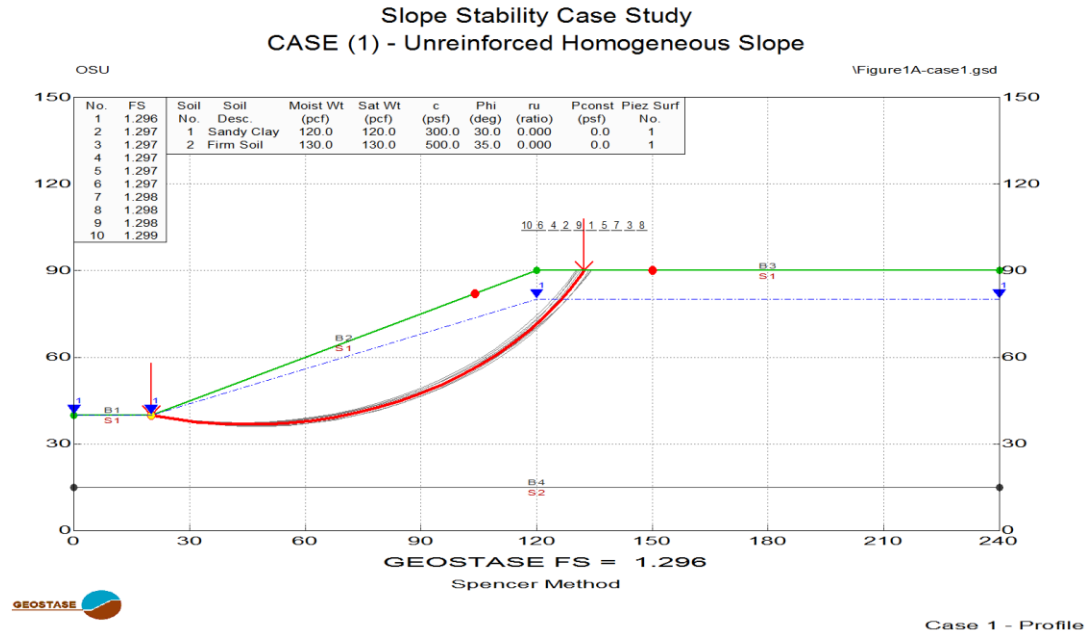


Figure 4.3: Plot of critical failure surfaces from GEOSTASE for case (1)

4.2.2 Analysis Results of Case (1) by FLAC

The shear strain increment at failure surface is shown in Figure 4.4, the mesh profile is shown in Figure 4.5, the total stresses are shown in Figure 4.6, the effective stresses are shown in Figure 4.7, the pore water pressures are shown in Figure 4.8, and the displacement directions are shown in Figure 4.9. The computed factor of safety was found as 1.25. The minimum value of factor of safety is less than 3% from that obtained from limit equilibrium method. However, the difference of computed factor of safety is relatively small. Additionally, the location of the failure surface is also close.

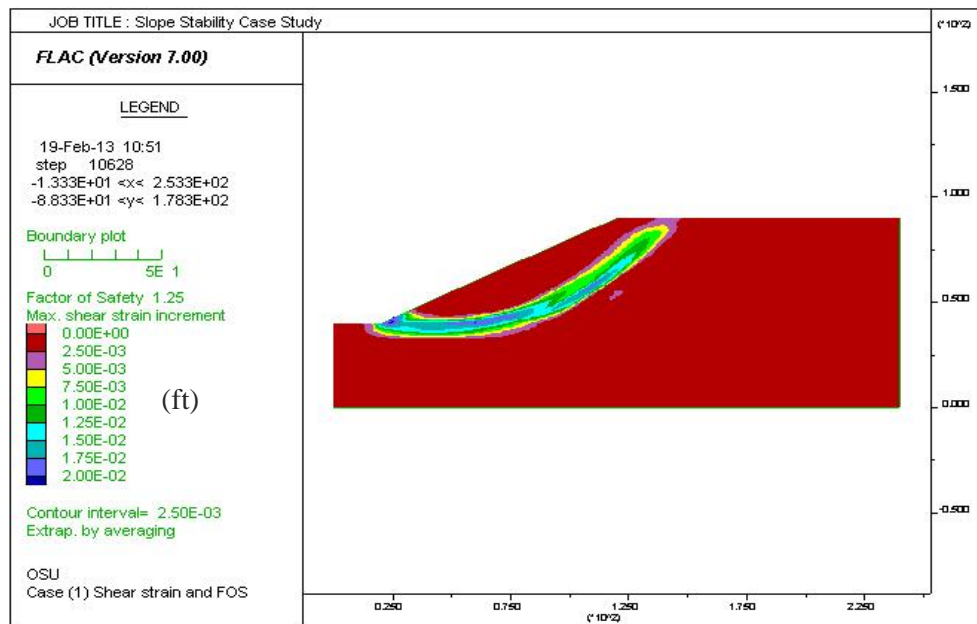


Figure 4.4: Shear strain plot and FS from FLAC for case (1)

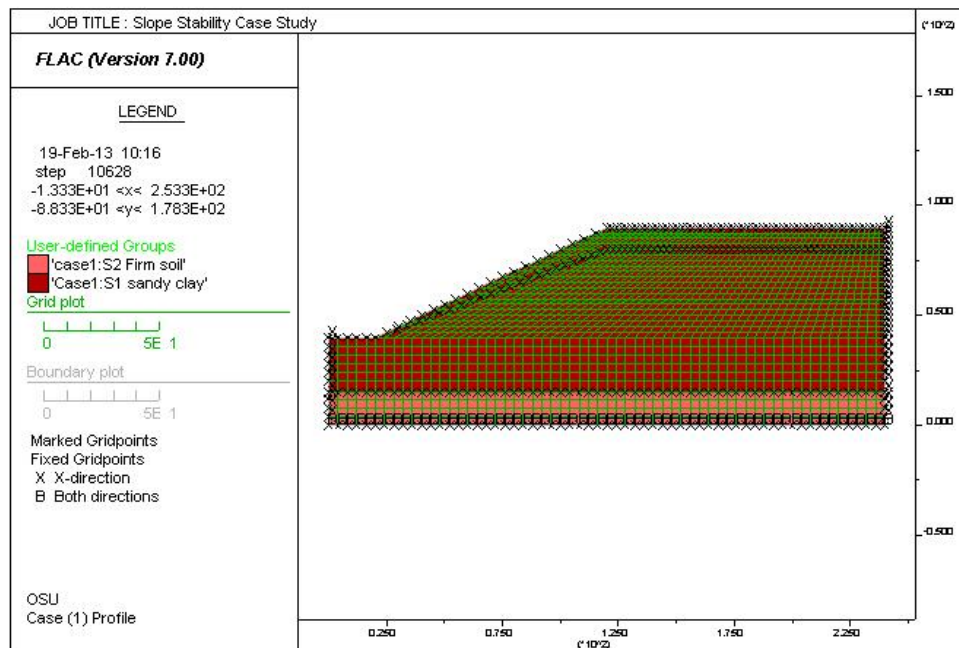


Figure 4.5: Mesh plot shows stress and strain quadrilateral element from FLAC for case (1)

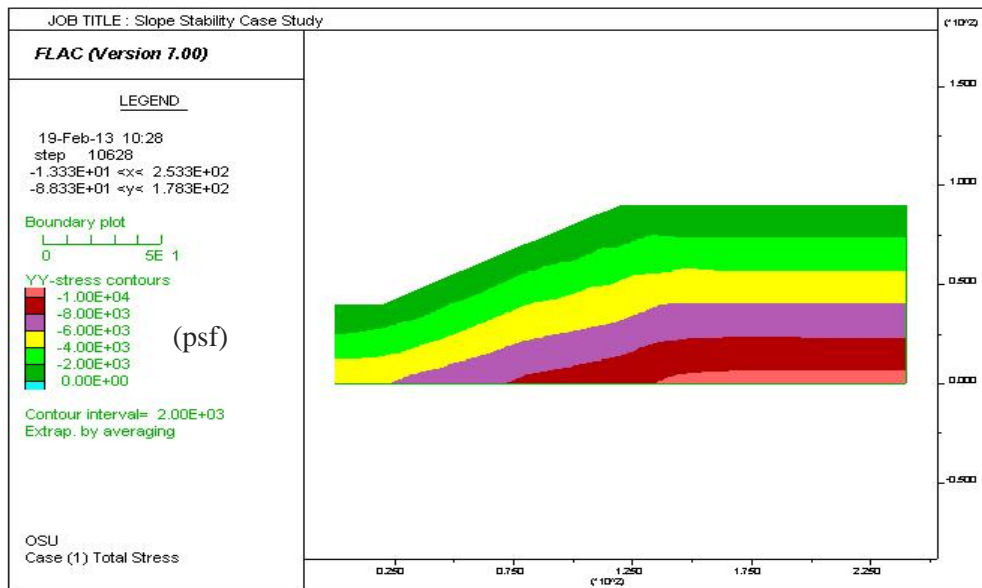


Figure 4.6: Contour plot for total stresses zones from FLAC for case (1)

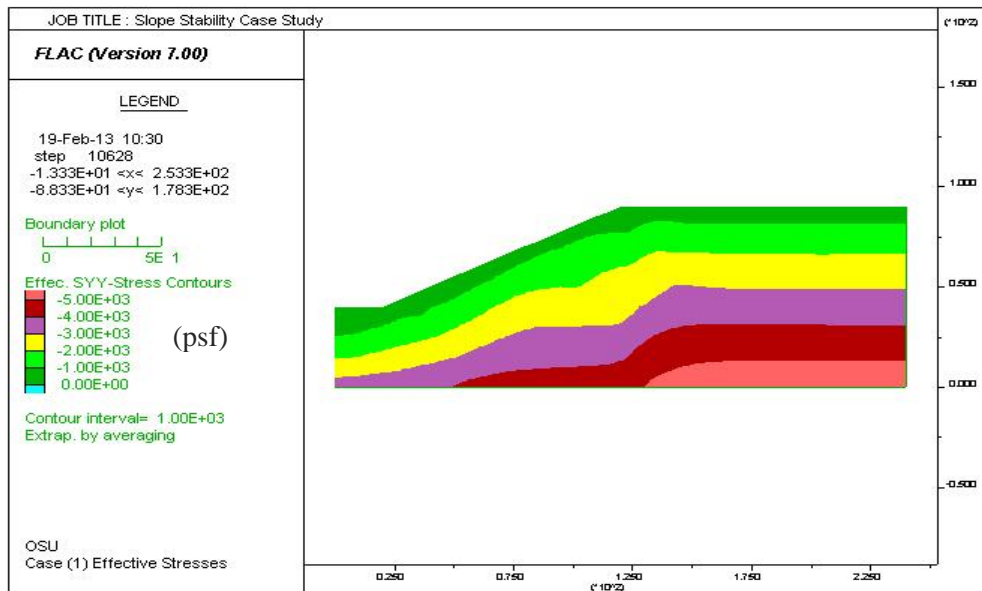


Figure 4.7: Contour plot for effective stresses zones from FLAC for case (1)

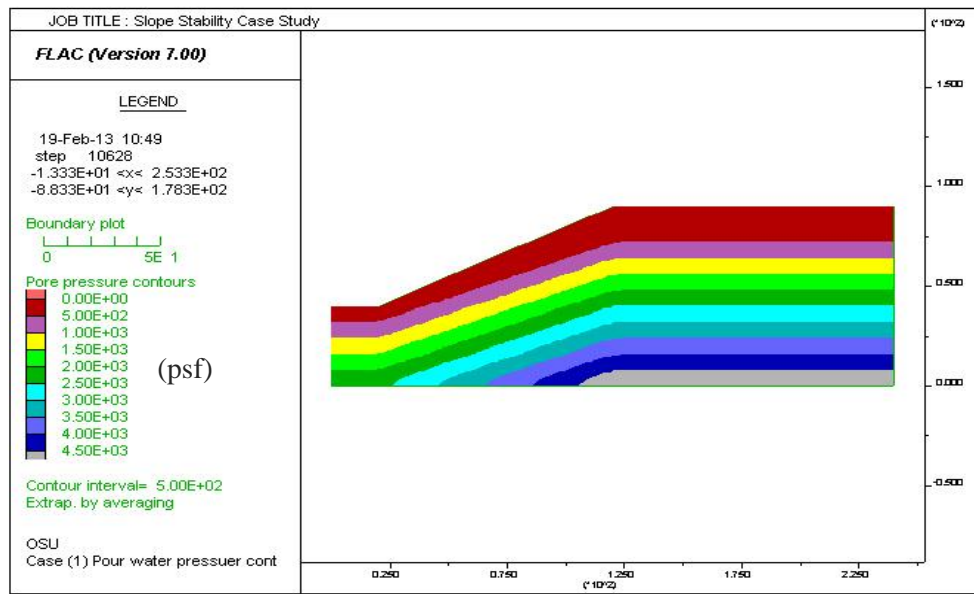


Figure 4.8: Contour plot for pore water pressure zones from FLAC for case (1)

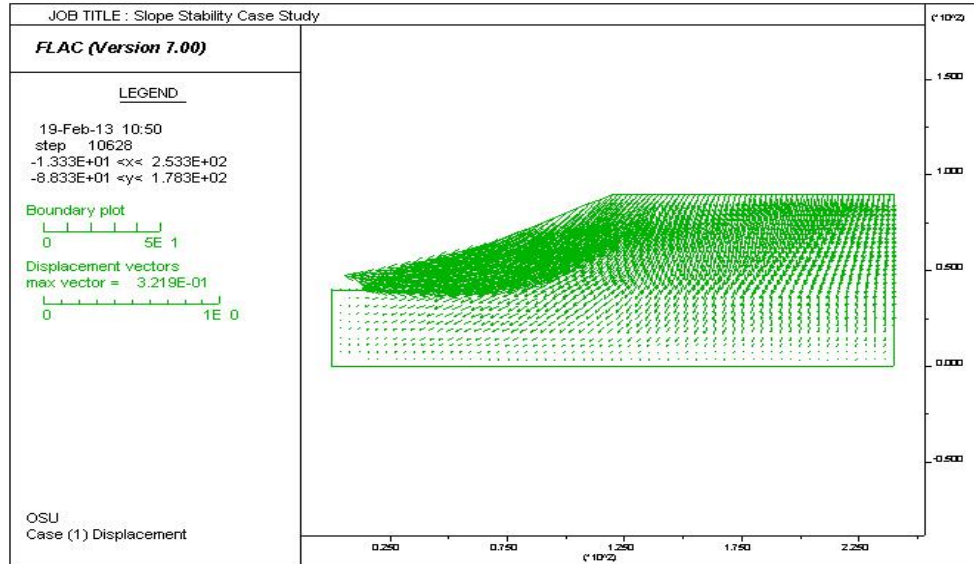


Figure 4.9: Displacement direction plot from FLAC for case (1)

4.2.3 Comparison

The radius from GEOSTASE was 97.782 ft., and the coordinates were found to be $x = 45.187$ ft and $y = 134.483$ ft. The same coordinates were depicted on the finite difference analysis of the slope shear strain increment in Figure 4.10.

Consistently, the result shows that the minimum values of factor of safety obtained from numerical analysis is less than 3% from limit equilibrium values. However, the difference of computed factor of safety is slightly lower but still within the acceptable range. The computed factor of safety and the failure surface were relatively close. Moreover, the shape of failure plane seems to be circular for both methods.

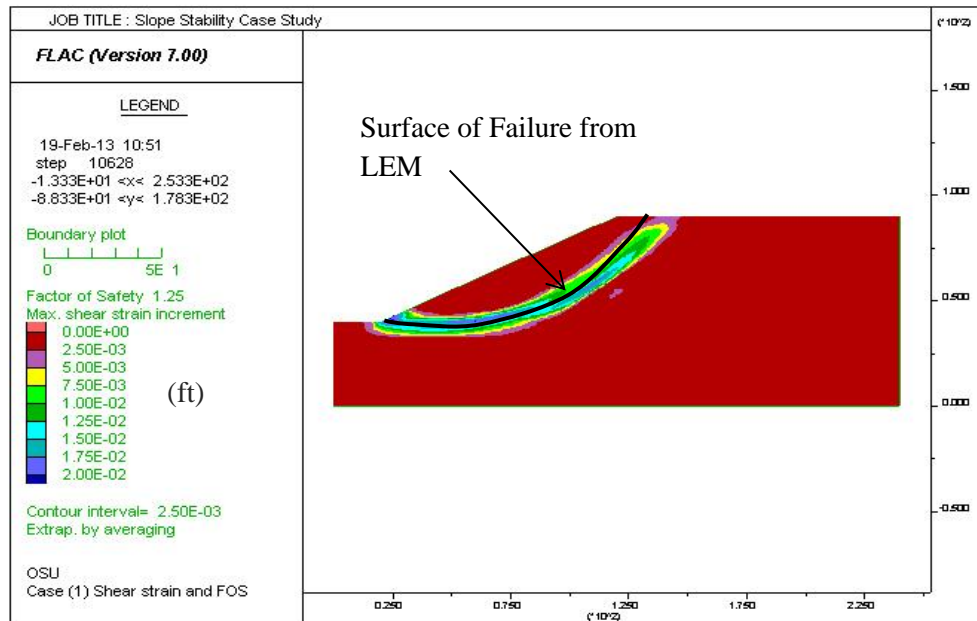


Figure 4.10: Critical surface from LEM depicted on shear strain from FDM for case (1)

4.3 Case (2): Non-Homogeneous with a Thin Weak Layer

The analysis results for both GEOSTASE with limit equilibrium based and FLAC with finite difference based method in this case are shown below.

4.3.1 Analysis Results of Case (2) by GEOSTASE

The Morgenstern and Price's method was used to solve the factor of safety because it works better with non-circular failure surfaces with a sharp edge. The geometry of the slope is shown in Figure 4.11. The output calculation of all surfaces of failure is shown in Figure 4.12. The analysis results of the critical surfaces of failure are shown in Figure 4.13. The output results of 10 most critical surfaces of failure are shown in Table 4.2. This is only 10 of most critical surface of failure which selected from total of 1000 surface analyzed. The minimum value of the factor of safety is 1.107. The surface of failure is non-circular.

Table 4.2: Computed factor of safety from GEOSTASE for case (2)

Failure Surface No.	Factor of Safety	Failure Surface Radius (ft)
1	1.107	N/A
2	1.116	N/A
3	1.116	N/A
4	1.121	N/A
5	1.125	N/A
6	1.137	N/A
7	1.137	N/A
8	1.138	N/A
9	1.140	N/A
10	1.141	N/A

Slope Stability Case Study
Case (2) Non homogeneous slope with high water level and weak layer

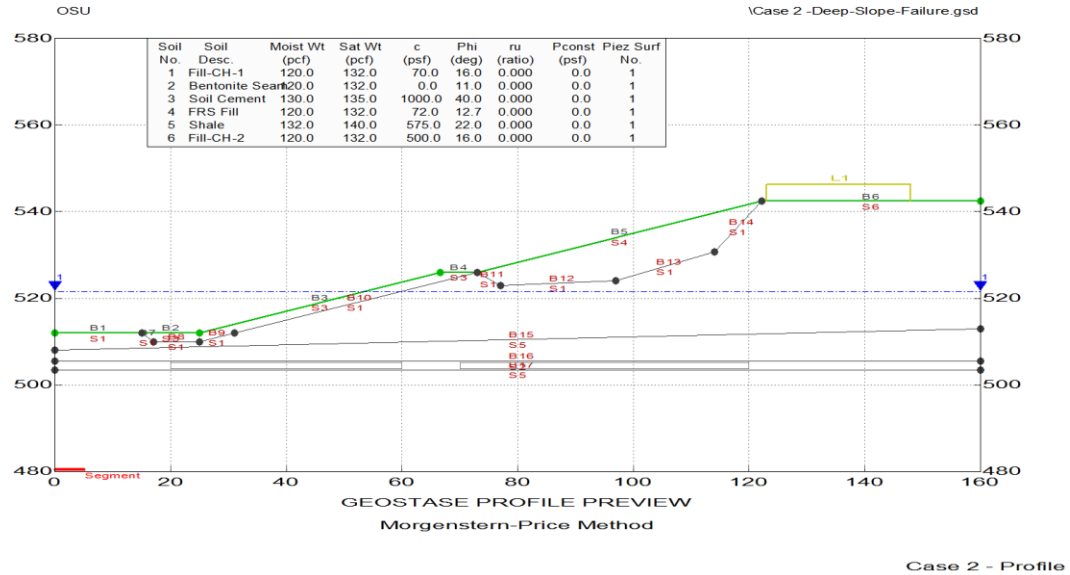


Figure 4.11: Profile preview from GEOSTASE for case (2)

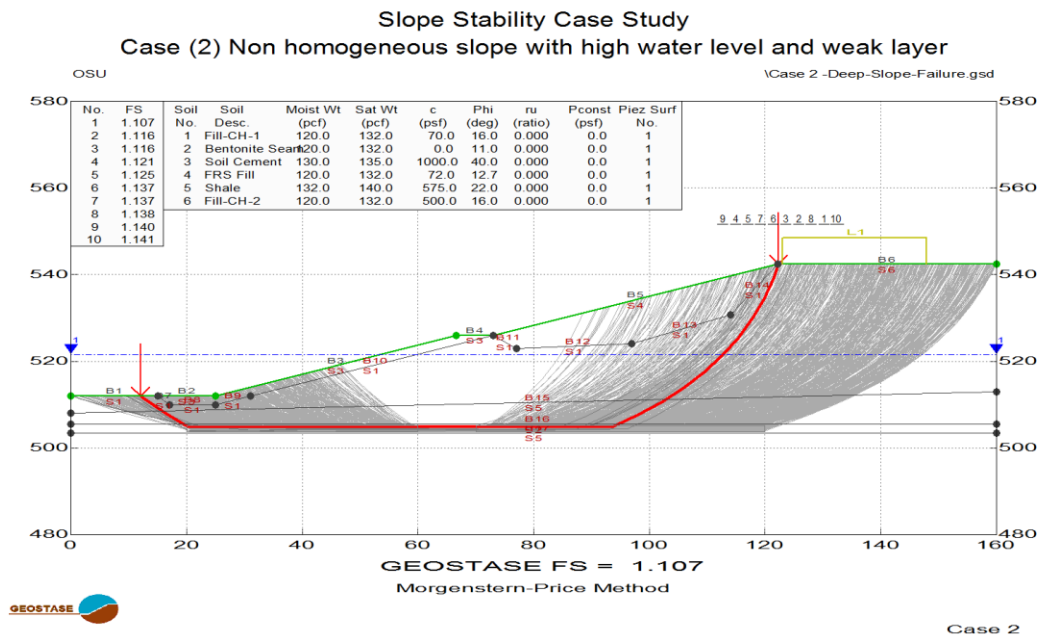


Figure 4.12: Plot of all failure of surfaces from GEOSTASE for case (2)

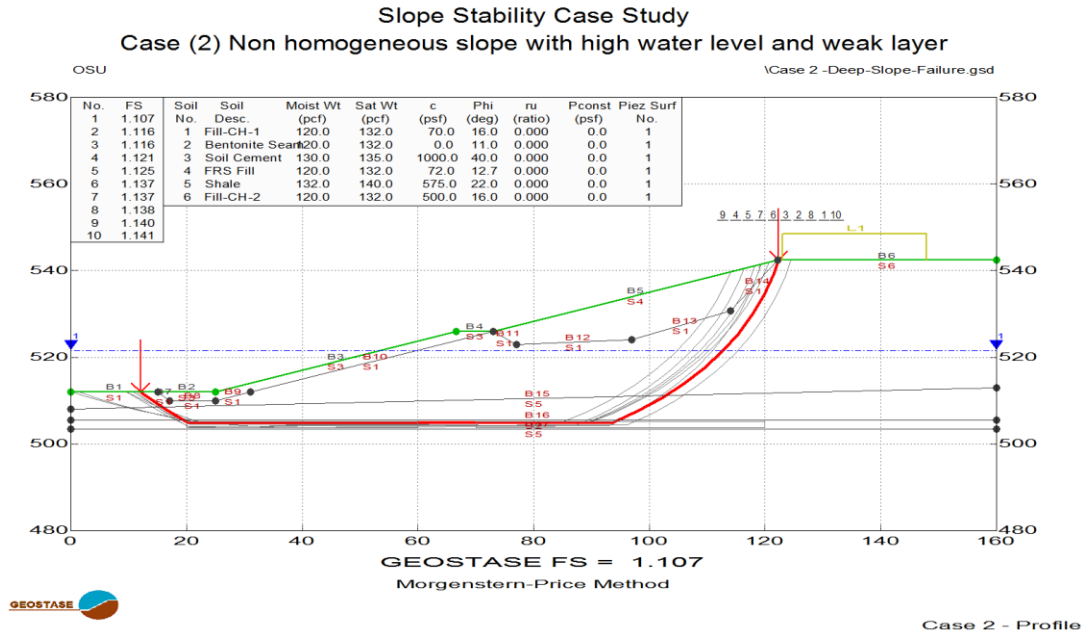


Figure 4.13: Plot of critical failure surfaces from GEOSTASE for case (2)

4.3.2 Analysis Results of Case (2) by FLAC

The shear strain increment at failure surface is shown in Figure 4.14, the mesh profile is shown in Figure 4.15, the total stresses are shown in Figure 4.16, the effective stresses are shown in Figure 4.17, the pore water pressures are shown in Figure 4.18, and the displacement directions are shown in Figure 4.19. The computed factor of safety was found as 1.08. The minimum value of factor of safety is less than 3% from that obtained from limit equilibrium method. However, the difference of computed factor of safety is relatively small. Additionally, the location of the failure surface is also closed.

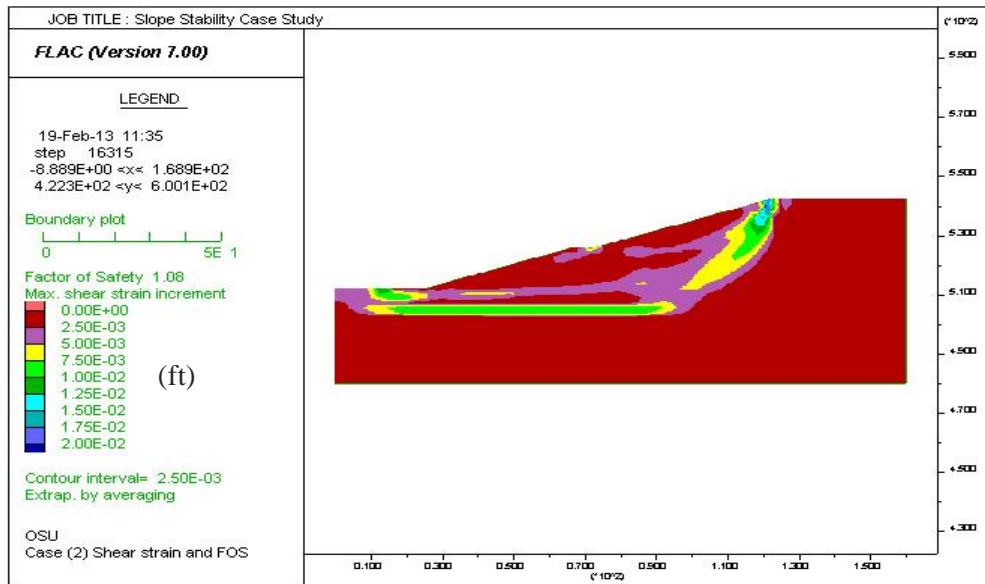


Figure 4.14: Shear strain plot (displacement) and FS from FLAC for case (2)

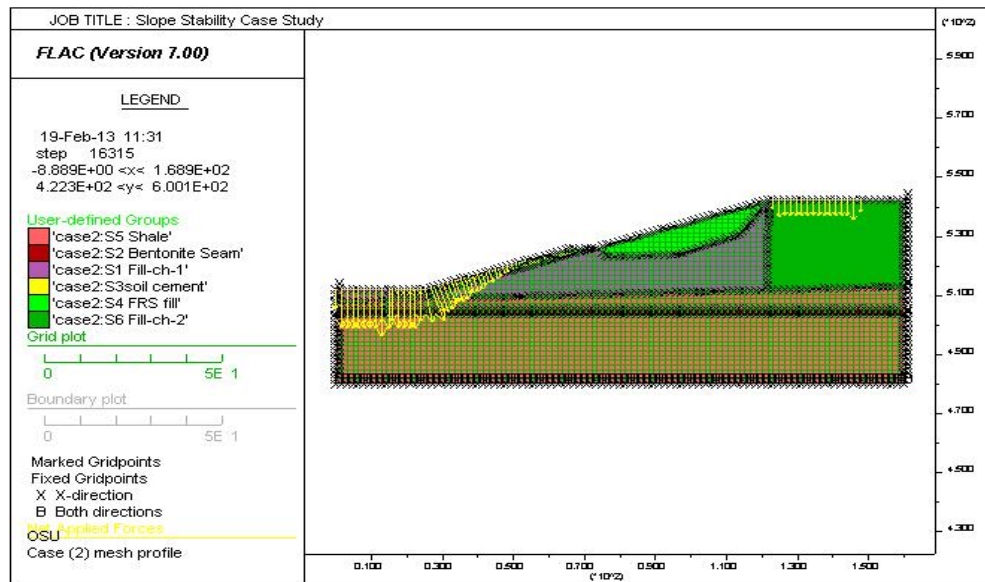


Figure 4.15: Mesh plot shows stress and strain quadrilateral element from FLAC for case (2)

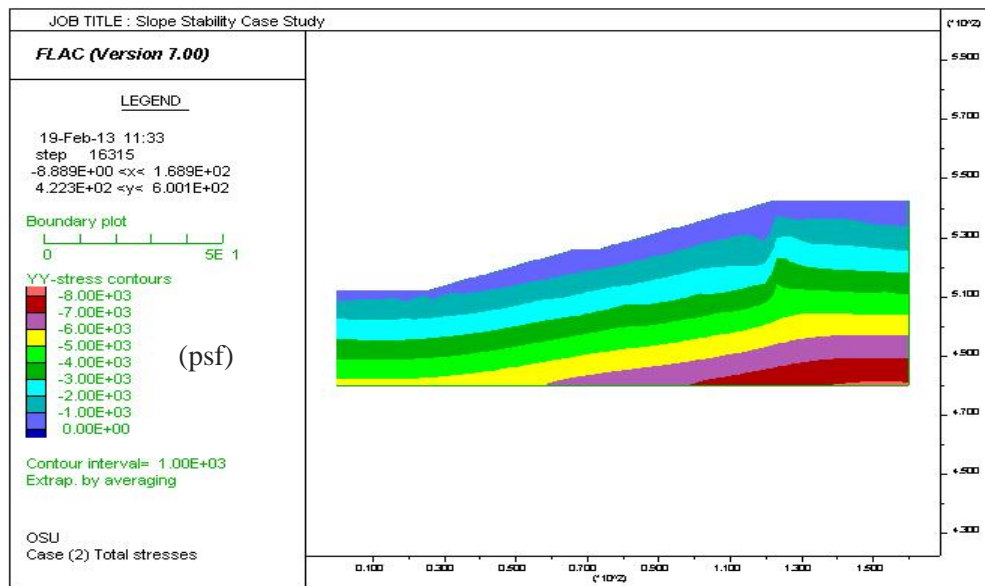


Figure 4.16: Contour plot for total stresses zones from FLAC for case (2)

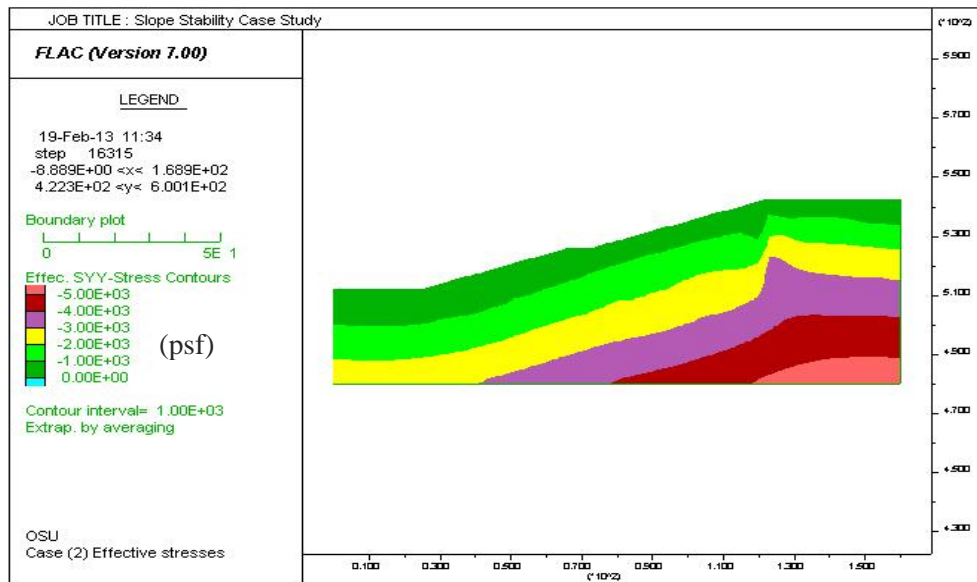


Figure 4.17: Contour plot for effective stresses zones from FLAC for case (2)

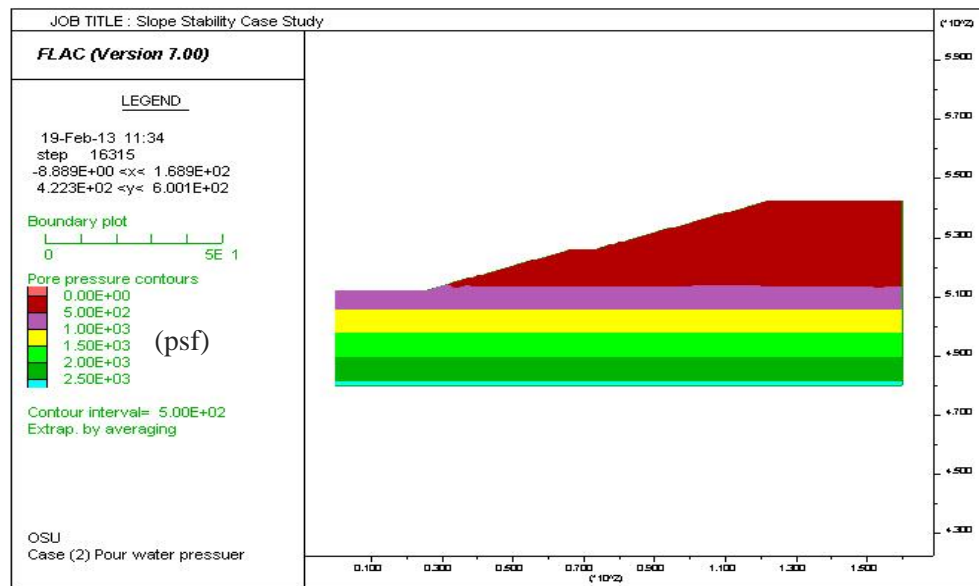


Figure 4.18: Contour plot for pore water pressure zones from FLAC for case (2)

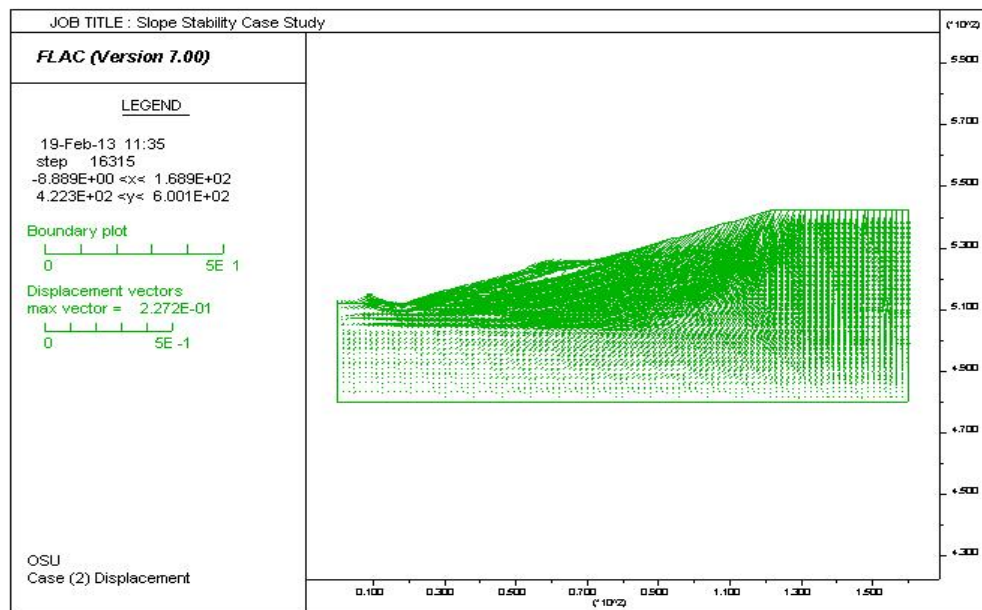


Figure 4.19: Displacement direction plot from FLAC for case (2)

4.3.3 Comparison

The same surface of failure obtained from limit equilibrium was depicted on the finite difference analysis of the slope shear strain increment in Figure 4.20.

Consistently, the results show that the minimum value of factor of safety obtained from numerical analysis is also less than by 3% from limit equilibrium value. And again, the difference of computed factor of safety is slightly lower but still within the acceptable range. The computed factor of safety and failure surface were still close. However, in the shape of failure plane seems to be non-circular for both methods as inspected to verge through the weak layer.

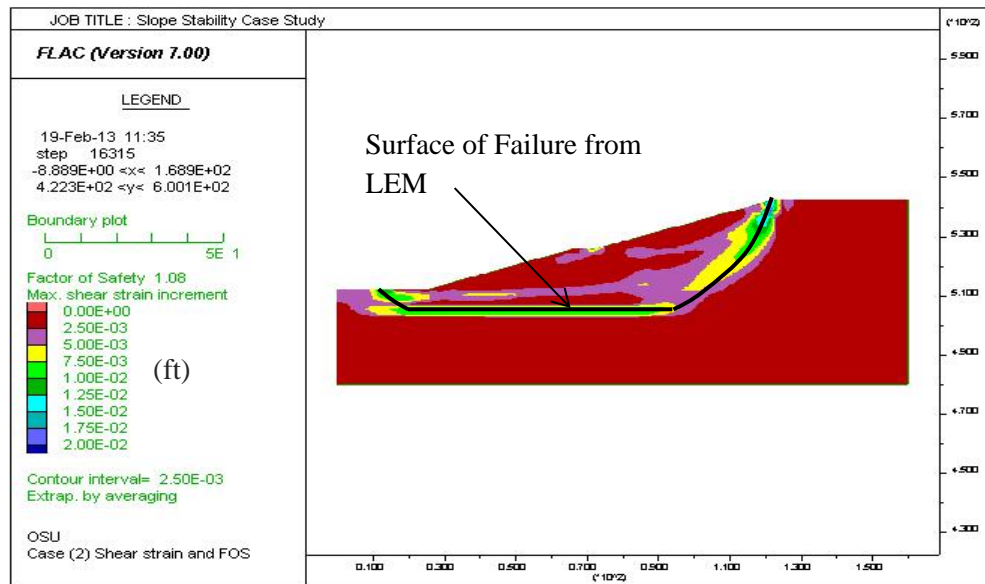


Figure 4.20: Critical surface from LEM depicted on shear strain from FDM for case (2)

4.4 Case (3): Levee Embankment Slope

The analysis results for both GEOSTASE with limit equilibrium based and FLAC with finite difference based method in this case are shown below.

4.4.1 Analysis Results of Case (3) by GEOSTASE

The Spencer method was used to solve the factor of safety. The geometry of the slope is shown in Figure 4.21. The output calculation of all surfaces of failure is shown in Figure 4.22.

The analysis results of the critical surfaces of failure are shown in Figure 4.23. The output results of 10 most critical surfaces of failure are shown in Table 4.3. This is only 10 of most critical surface of failure which selected from total of 1000 surface analyzed. The minimum value of the factor of safety is 1.188 at failure surface circle center coordinate $x = 44.855$ ft and $y = 62.667$ ft with radius of 58.231ft.

Table 4.3: Computed factor of safety from GEOSTASE for case (3)

Failure Surface No.	Factor of Safety	Failure Surface Radius (ft)
1	1.188	58.231
2	1.189	59.624
3	1.189	57.256
4	1.191	54.871
5	1.191	59.935
6	1.191	61.349
7	1.191	57.716
8	1.192	56.571
9	1.192	63.110
10	1.193	62.903

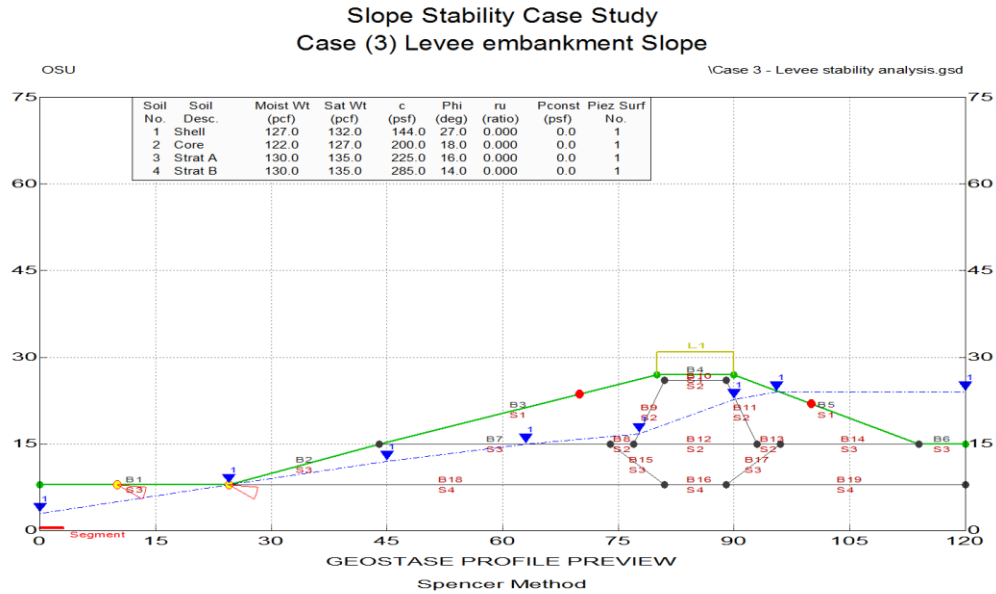


Figure 4.21: Profile preview from GEOSTASE for case (3)

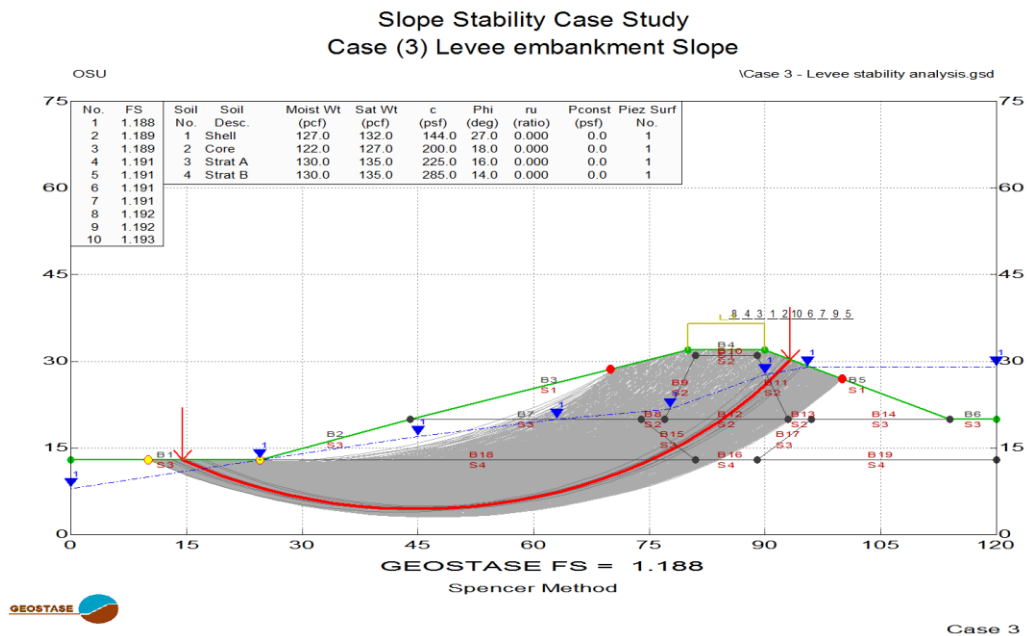


Figure 4.22: Plot of all failure of surfaces from GEOSTASE for case (3)

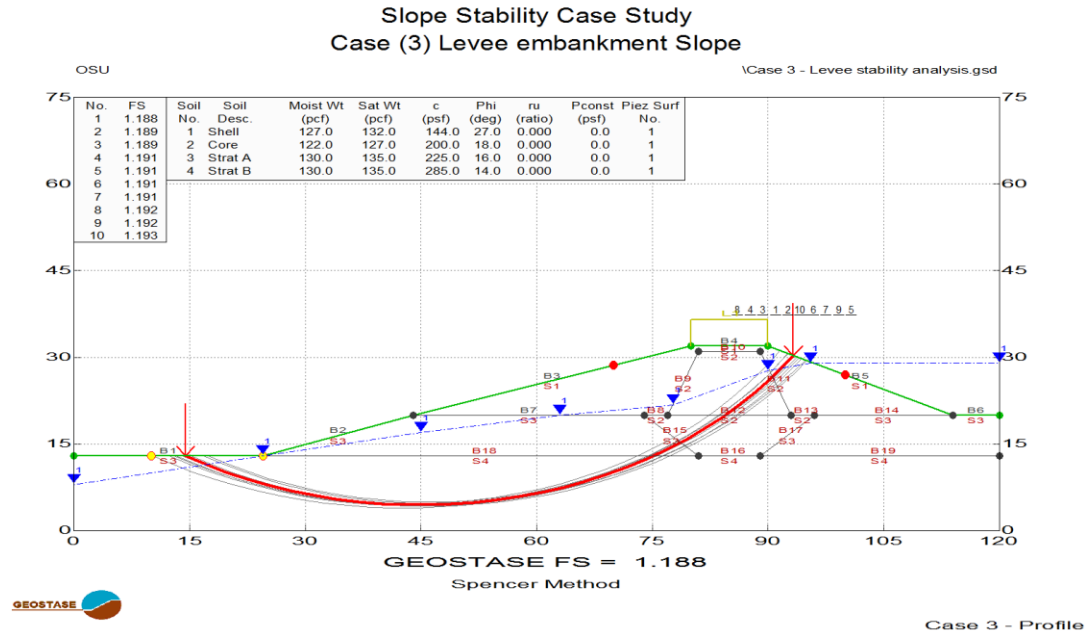


Figure 4.23: Plot of critical failure surfaces from GEOSTASE for case (3)

4.4.2 Analysis Results of Case (3) by FLAC

The shear strain increment at failure surface is shown in Figure 4.24, the mesh profile is shown in Figure 4.25, the total stresses are shown in Figure 4.26, the effective stresses are shown in Figure 4.27, the pore water pressures are shown in Figure 4.28, and the displacement directions are shown in Figure 4.29. The computed factor of safety was found as 1.19. The minimum value of factor of safety is equal the factor of safety obtained from limit equilibrium method. However, the location of the failure surface is also relatively closed.

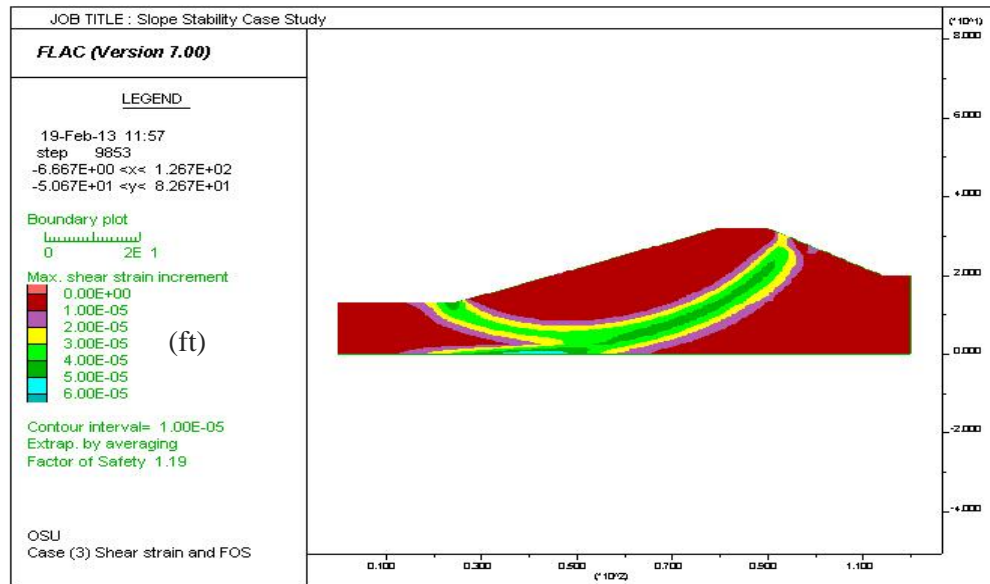


Figure 4.24: Shear strain plot (displacement) and FS from FLAC for case (3)

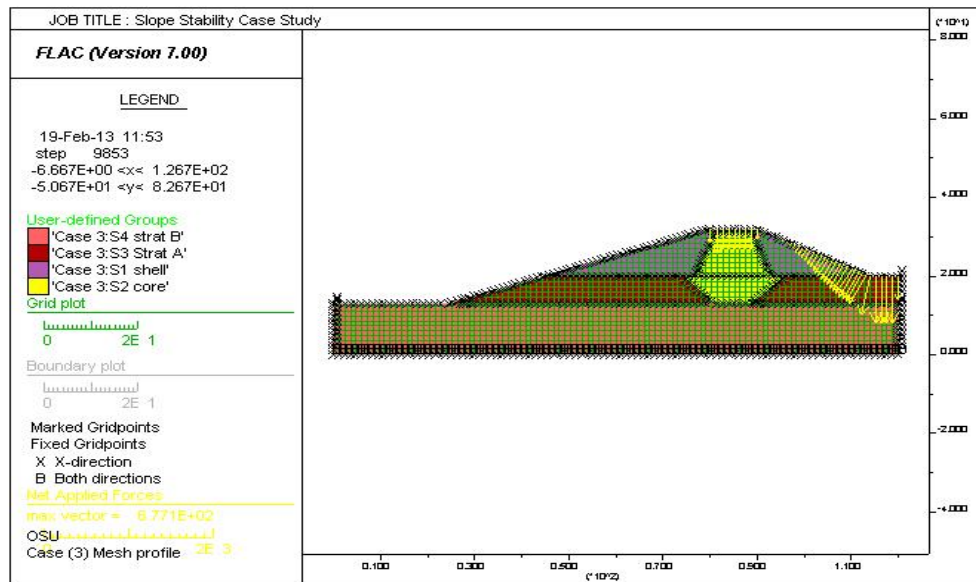


Figure 4.25: Mesh plot shows stress and strain quadrilateral element from FLAC for case (3)

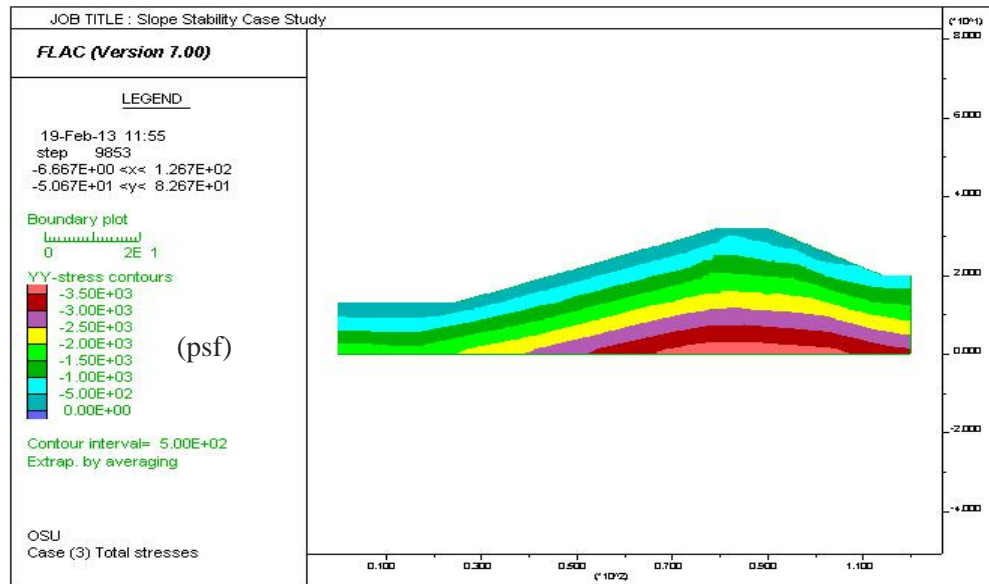


Figure 4.26: Contour plot for total stresses zones from FLAC for case (3)

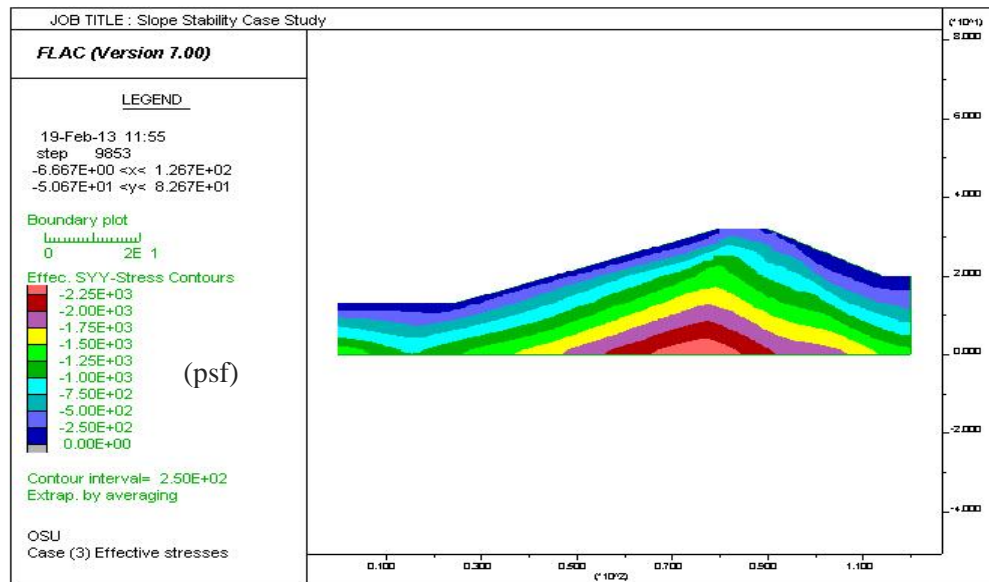


Figure 4.27: Contour plot for effective stresses zones from FLAC for case (3)

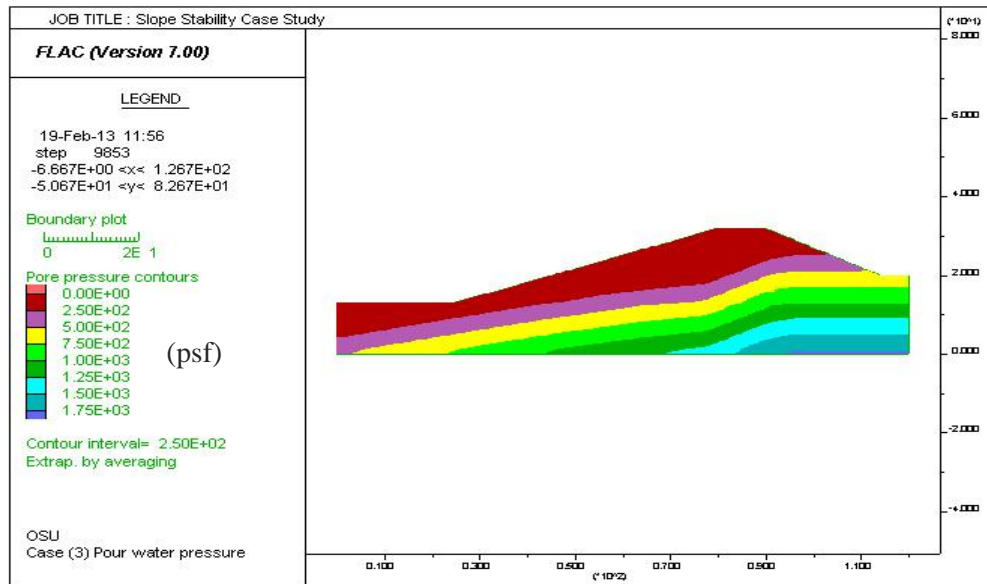


Figure 4.28: Contour plot for pore water pressure zones from FLAC for case (3)

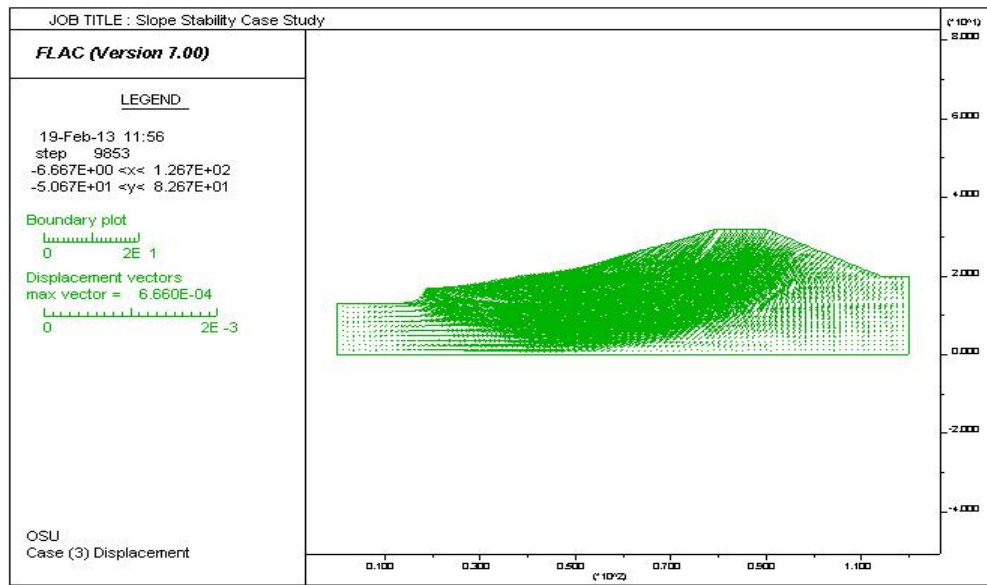


Figure 4.29: Displacement direction plot from FLAC for case (3)

4.4.3 Comparison

The same surface of failure obtained from limit equilibrium was depicted on the finite difference analysis of the slope shear strain increment in Figure 4.30.

Consistently, the result shows that the minimum values of factor of safety obtained from numerical analysis is equal to the minimum factor of safety value from limit equilibrium method. Although, the computed factor of safety was equal to limit equilibrium value, the failure surface is slightly different. Moreover, the shape of failure plane seems to be circular for both methods.

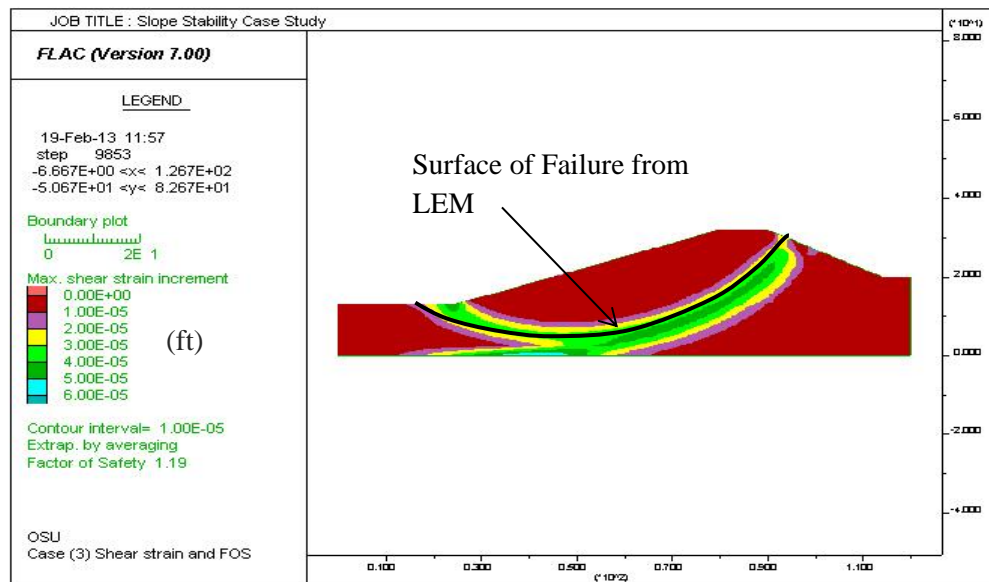


Figure 4.30: Critical surface from LEM depicted on shear strain from FDM for case (3)

4.5 Case (4): Deep Slope with a Storage Tank

The analysis results for both GEOSTASE with limit equilibrium based and FLAC with finite difference based method in this case are shown below.

4.5.1 Analysis Results of Case (4) by GEOSTASE

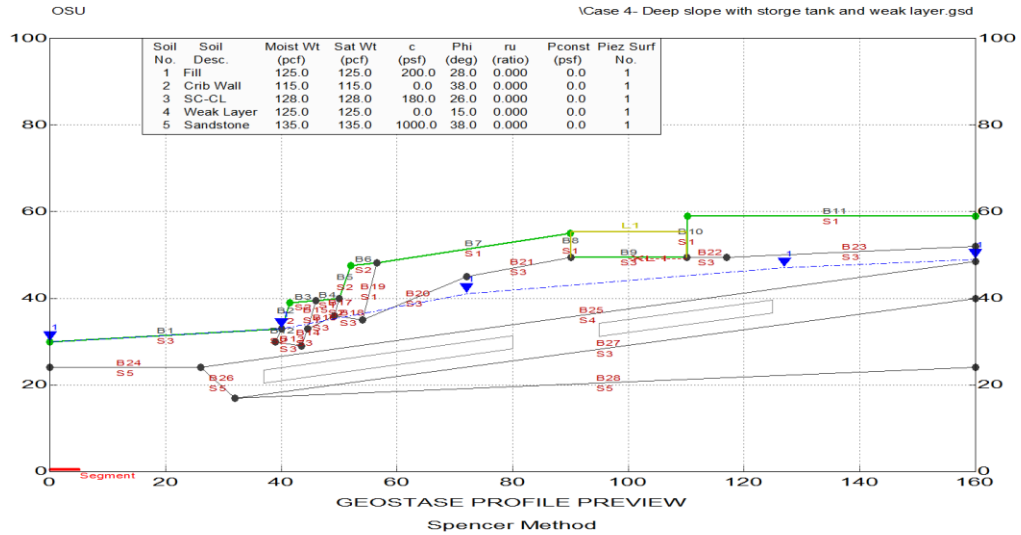
The Spencer method was used to solve the factor of safety. The geometry of the slope is shown in Figure 4.31. The output calculation of all surfaces of failure is shown in Figure 4.32.

The analysis results of the critical surfaces of failure are shown in Figure 4.33. The output results of 10 most critical surfaces of failure are shown in Table 4.4. This is only 10 of most critical surface of failure which selected from total of 1000 surface analyzed. The minimum value of the factor of safety is 1.005.

Table 4.4: Computed factor of safety from GEOSTASE for case (4)

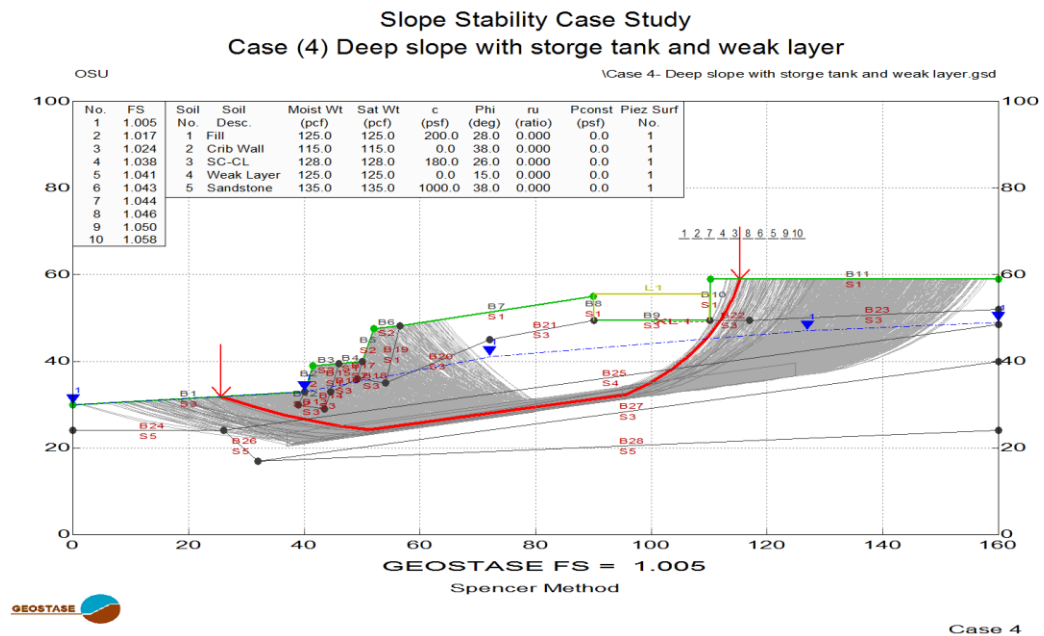
Failure Surface No.	Factor of Safety	Failure Surface Radius (ft)
1	1.005	N/A
2	1.017	N/A
3	1.024	N/A
4	1.038	N/A
5	1.041	N/A
6	1.043	N/A
7	1.044	N/A
8	1.046	N/A
9	1.050	N/A
10	1.058	N/A

Slope Stability Case Study Case (4) Deep slope with storage tank and weak layer



Case 4 - Profile

Figure 4.31: Profile preview from GEOSTASE for case (4)



Case 4

Figure 4.32: Plot of all failure of surfaces from GEOSTASE for case (4)

Slope Stability Case Study Case (4) Deep slope with storage tank and weak layer

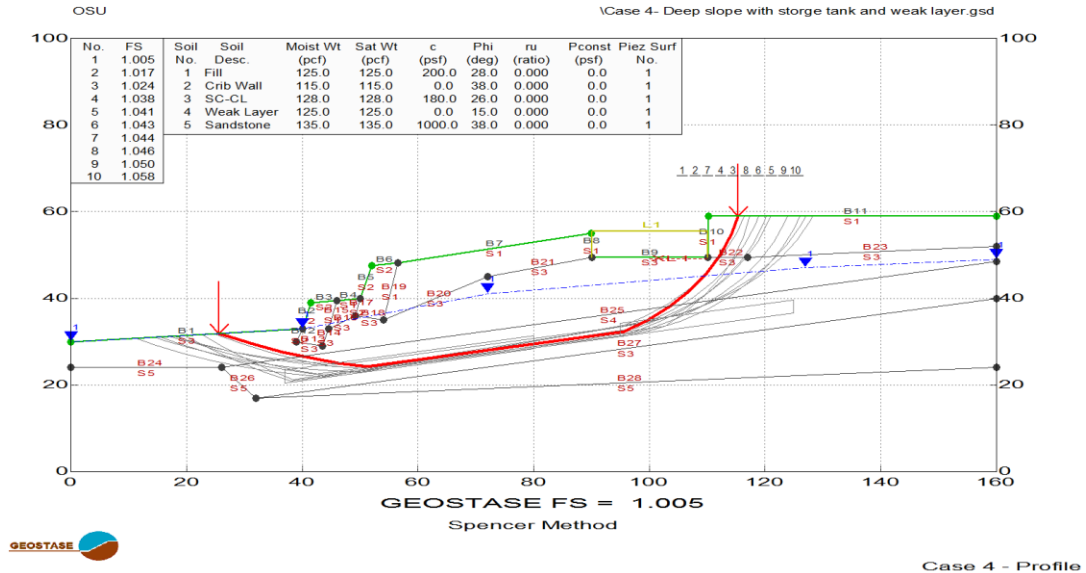


Figure 4.33: Plot of critical failure surfaces from GEOSTASE for case (4)

4.5.2 Analysis Results of Case (4) by FLAC

The shear strain increment at failure surface is shown in Figure 4.34, the mesh profile is shown in Figure 4.35, the total stresses are shown in Figure 4.36, the effective stresses are shown in Figure 4.37, the pore water pressures are shown in Figure 4.38, and the displacement directions are shown in Figure 4.39. The computed factor of safety was found as 0.9. The minimum value of factor of safety is less than 11% from that obtained from limit equilibrium method. In this case, the difference of computed factor of safety is relatively high and considerable. However, the location of the failure surface is slightly different.

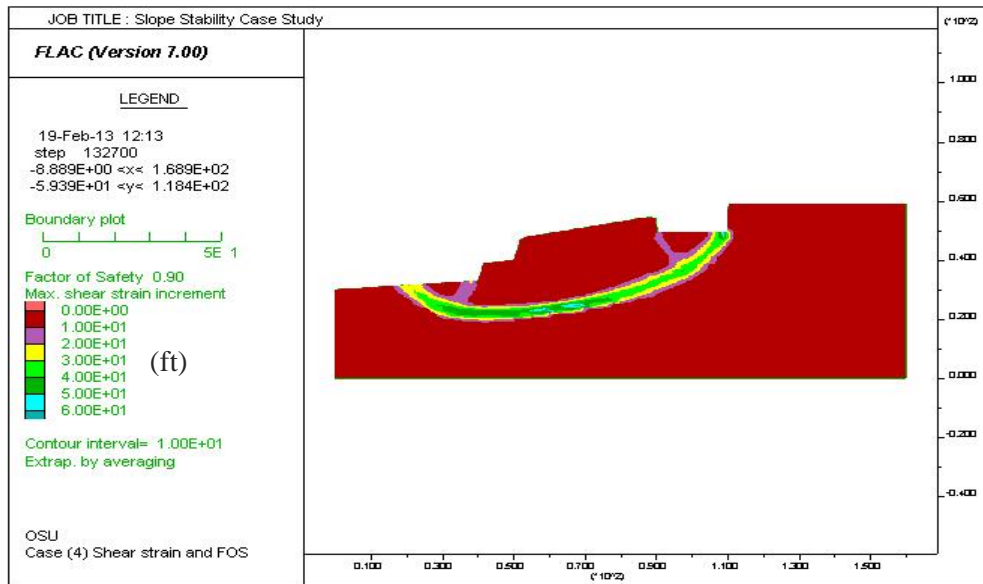


Figure 4.34: Shear strain plot (displacement) and FS from FLAC for case (4)

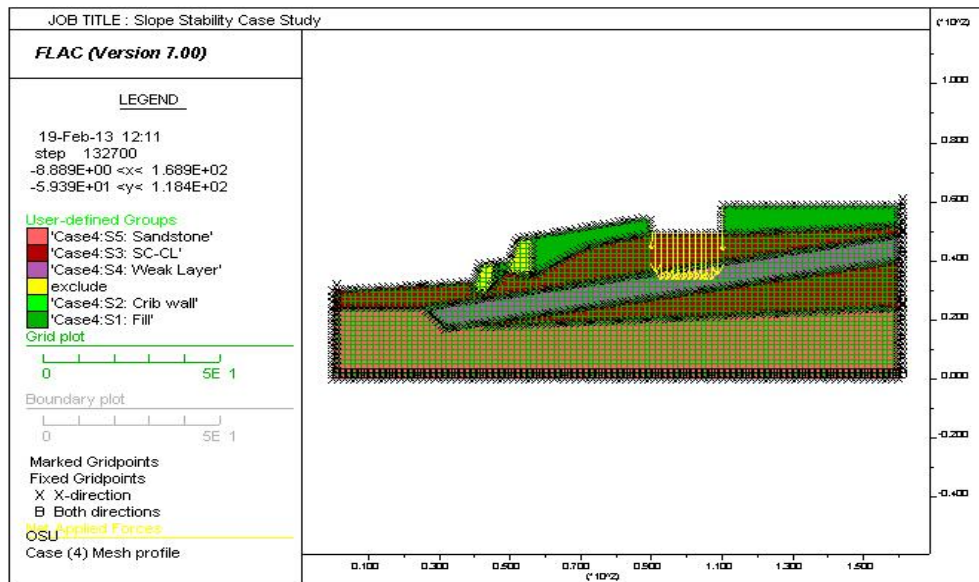


Figure 4.35: Mesh plot shows stress and strain quadrilateral element from FLAC for case (4)

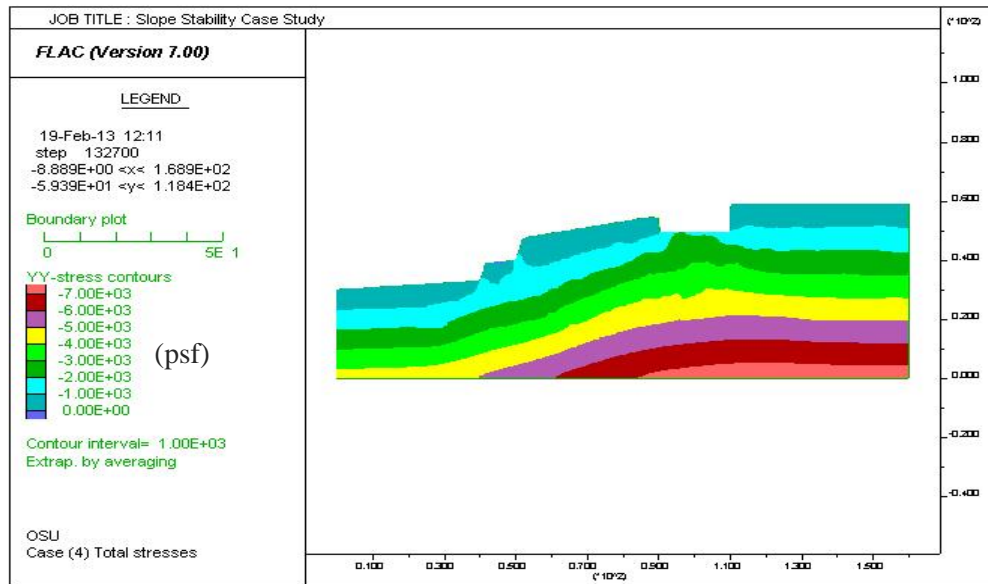


Figure 4.36: Contour plot for total stresses zones from FLAC for case (4)

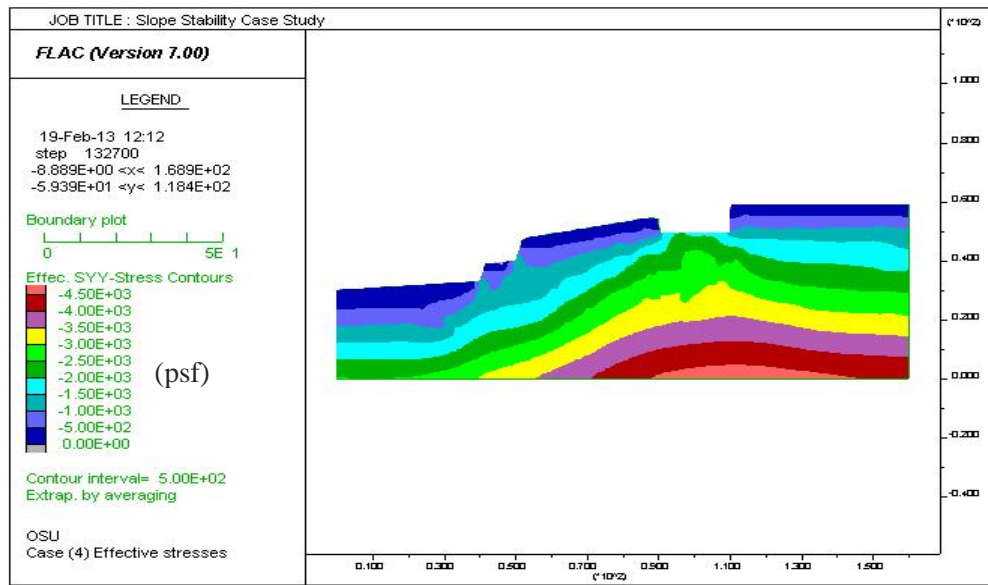


Figure 4.37: Contour plot for effective stresses zones from FLAC for case (4)

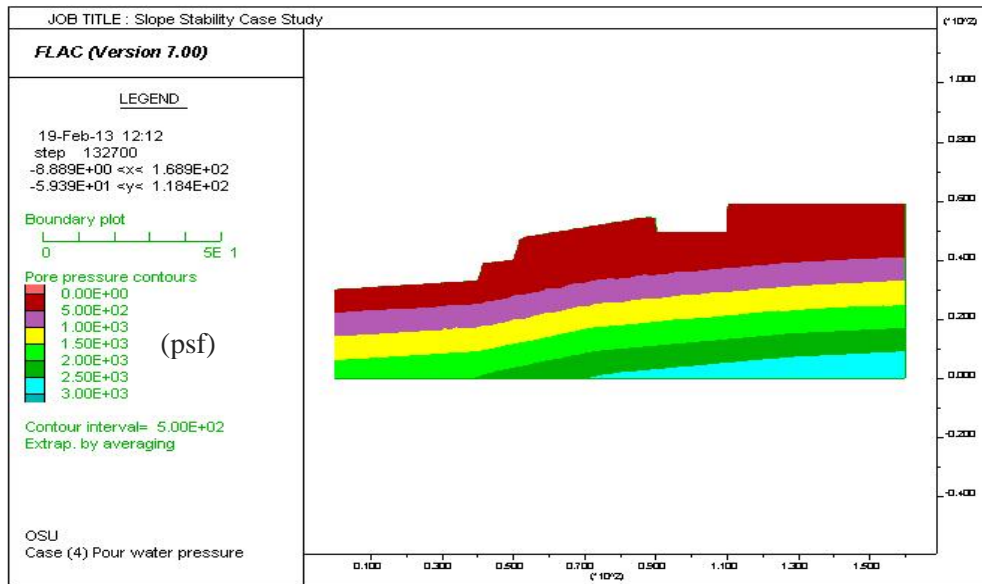


Figure 4.38: Contour plot for pore water pressure zones from FLAC for case (4)

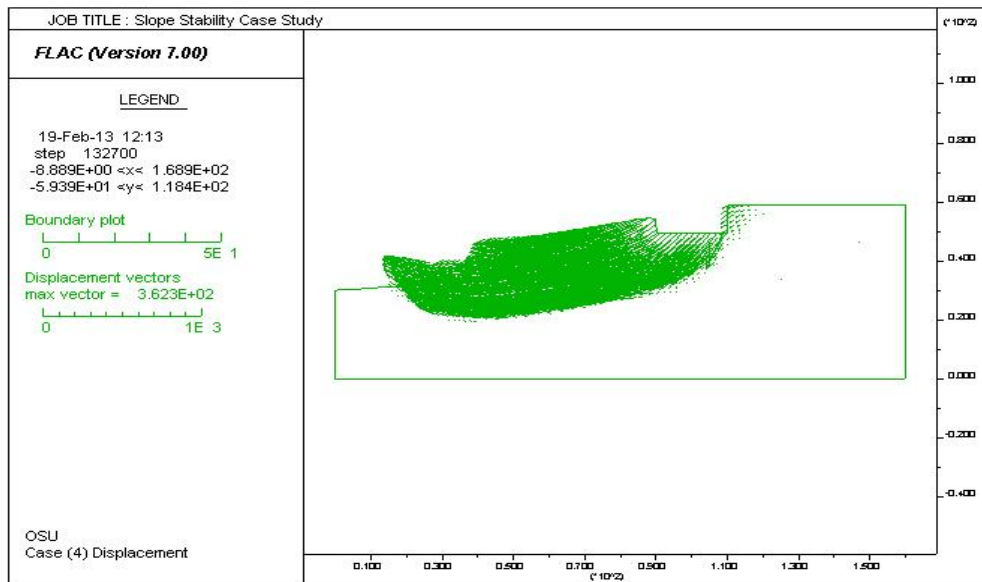


Figure 4.39: Displacement direction plot from FLAC for case (4)

4.5.3 Comparison

The same surface of failure obtained from limit equilibrium was depicted on the finite difference analysis of the slope shear strain increment in Figure 4.40.

Consistently, the result shows that the minimum value of factor of safety obtained from numerical analysis is less than 11% from limit equilibrium value. The difference of computed factor of safety is slightly different but both methods shows that the slope in the failure condition. The failure surface is slightly different due to an arbitrary partitioning of the critical surface from LEM. Moreover, the shape of failure plane seems to be non-circular for both methods following the weak layer.

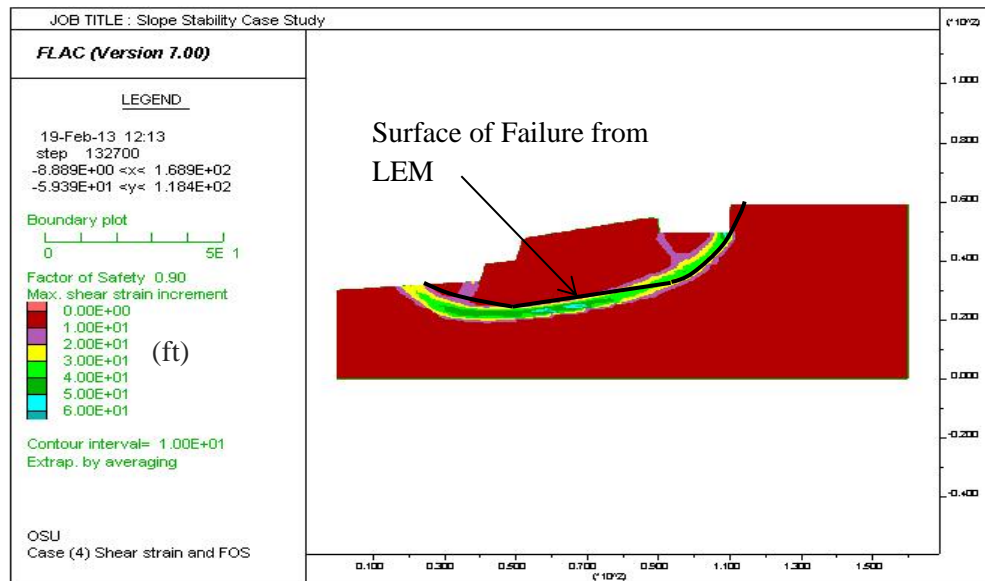


Figure 4.40: Critical surface from LEM depicted on shear strain from FDM for case (4)

4.6 Case (5): MSE Wall Reinforced with Soil Nails

The analysis results for both GEOSTASE with limit equilibrium based and FLAC with finite difference based method in this case are shown below.

4.6.1 Analysis Results of Case (5) by GEOSTASE

The Spencer method was used to solve the factor of safety. The geometry of the slope is shown in Figure 4.41. The output calculation of all surfaces of failure is shown in Figure 4.42. The analysis results of the critical surfaces of failure are shown in Figure 4.43. The output results of 10 most critical surfaces of failure are shown in Table 4.5. This is only 10 of most critical surface of failure which selected from total of 1000 surface analyzed. The minimum value of the factor of safety is 1.335 at failure surface circle center coordinate $x = -36.717$ ft and $y = 1173.854$ ft with radius of 199.908 ft.

Table 4.5: Computed factor of safety from GEOSTASE for case (5)

Failure Surface No.	Factor of Safety	Failure Surface Radius (ft)
1	1.335	199.908
2	1.335	200.002
3	1.335	200.002
4	1.336	199.872
5	1.336	199.872
6	1.337	199.811
7	1.337	184.082
8	1.337	184.082
9	1.338	199.894
10	1.338	199.981

SLOPE STABILITY CASE STUDY **Case (5) MSE Wall Modeled with Soil Nails**

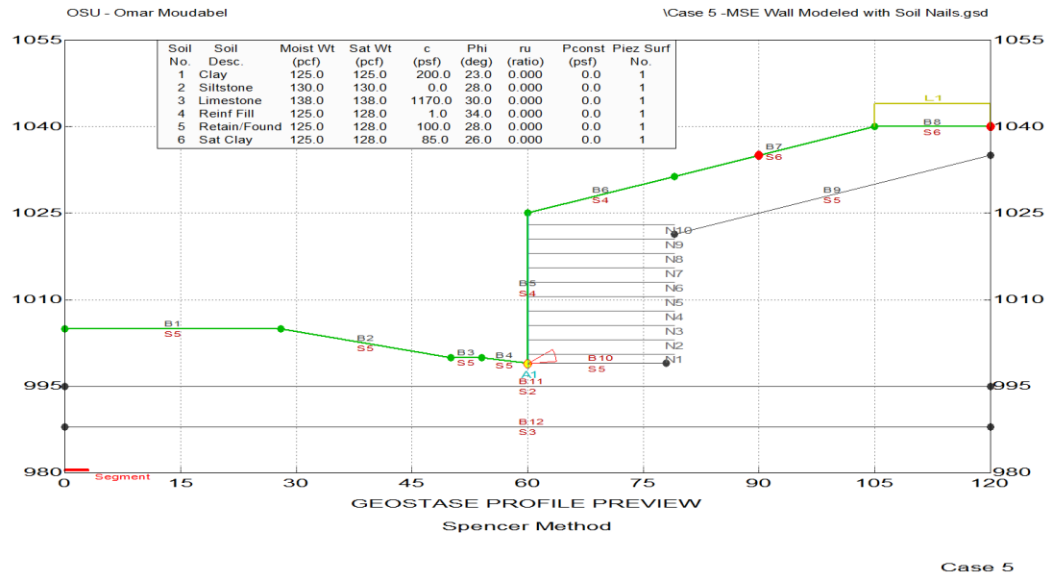


Figure 4.41: Profile preview from GEOSTASE for case (5)

SLOPE STABILITY CASE STUDY **Case (5) MSE Wall Modeled with Soil Nails**

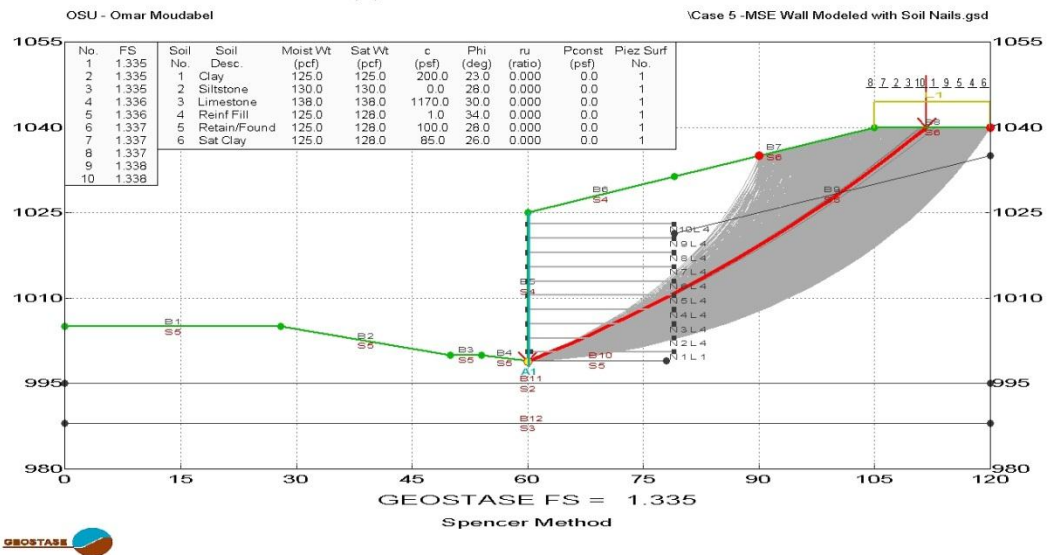


Figure 4.42: Plot of all failure surfaces from GEOSTASE for case (5)

SLOPE STABILITY CASE STUDY Case (5) MSE Wall Modeled with Soil Nails

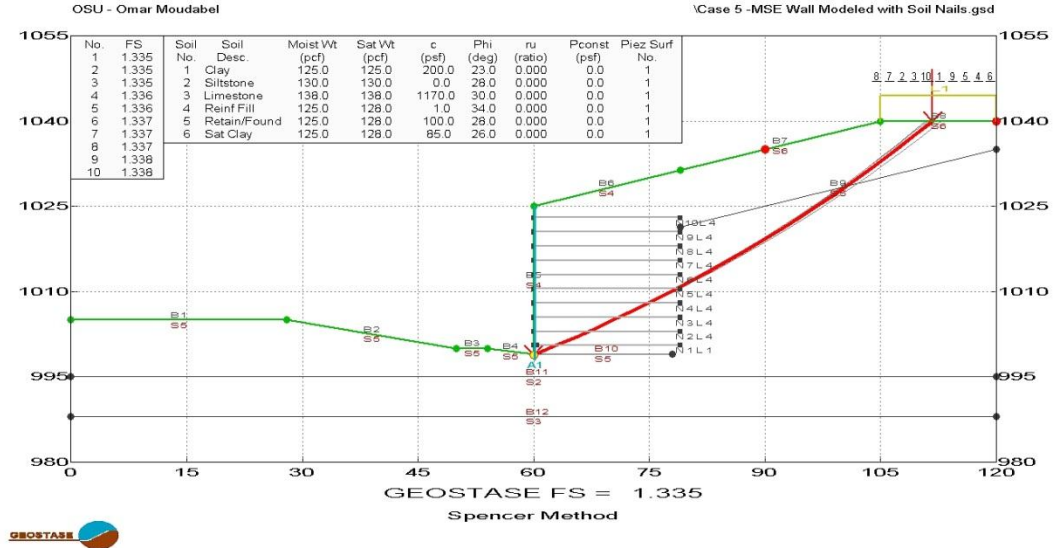


Figure 4.43: Plot of critical failure surfaces from GEOSTASE for case (5)

4.6.2 Analysis Results of Case (5) by FLAC

The shear strain increment at failure surface is shown in Figure 4.44, the mesh profile is shown in Figure 4.45, the total stresses are shown in Figure 4.46, and the displacement directions are shown in Figure 4.47. The computed factor of safety was found as 1.34. The minimum value of factor of safety is equal the factor of safety obtained from limit equilibrium method. However, the location of the failure surface is quite different.

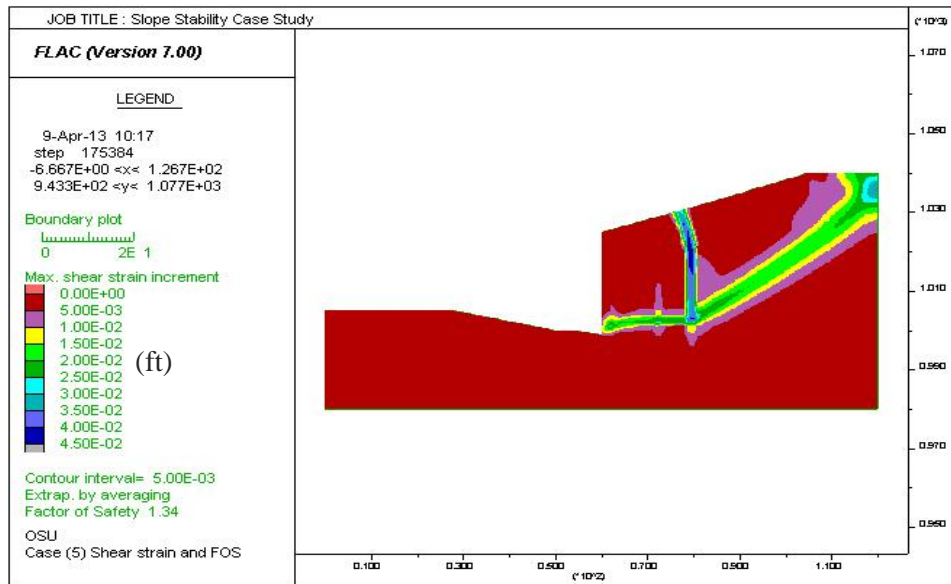


Figure 4.44: Shear strain plot (displacement) and FS from FLAC for case (5)

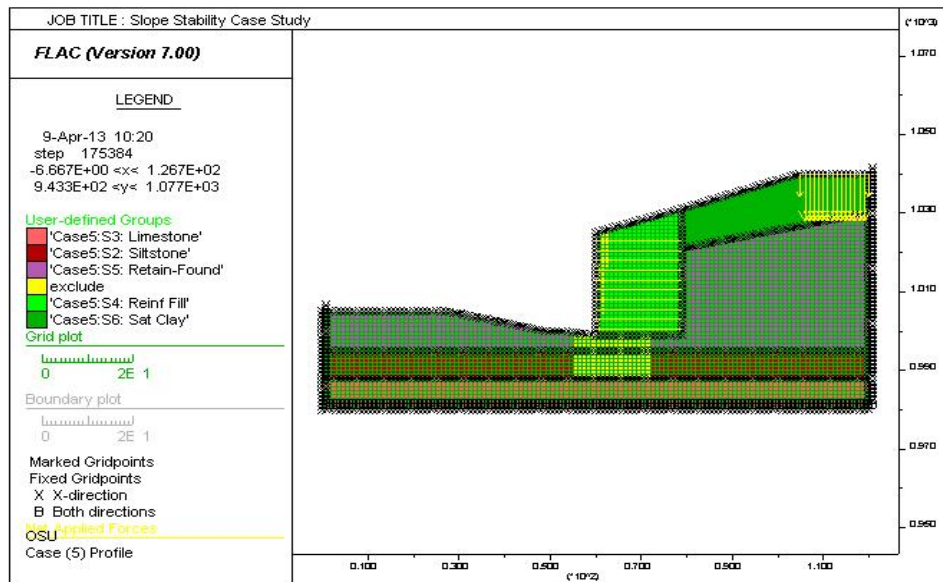


Figure 4.45: Mesh plot shows stress and strain quadrilateral element from FLAC for case (5)

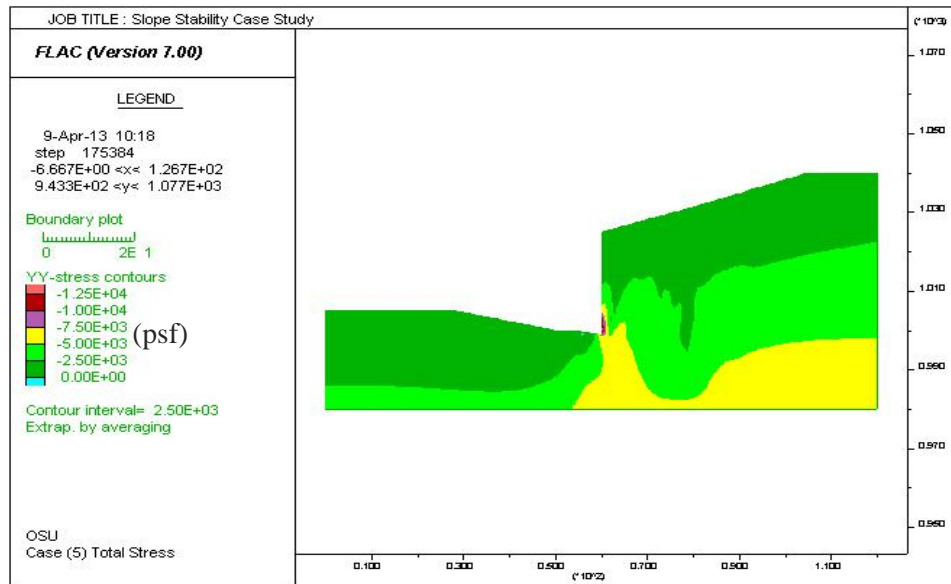


Figure 4.46: Contour plot for total stresses zones from FLAC for case (5)

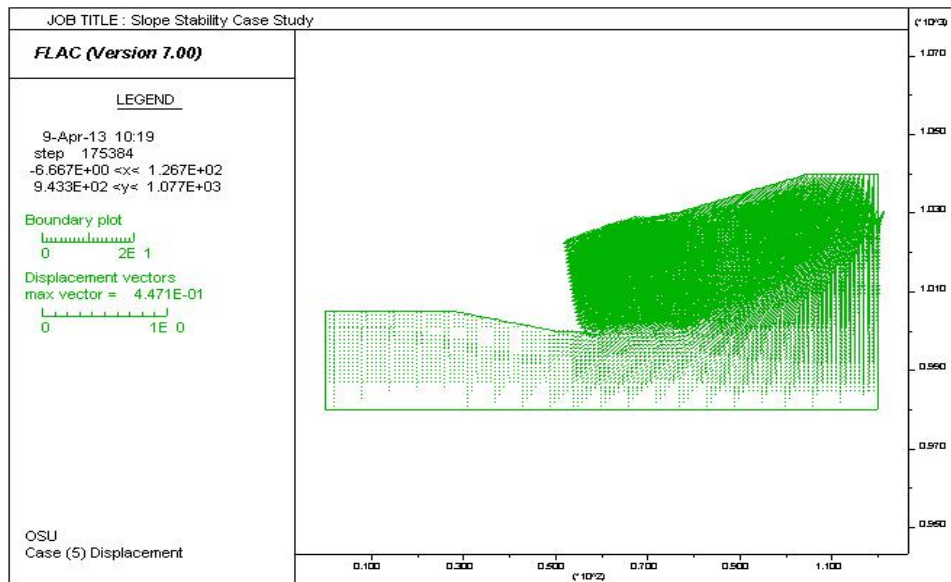


Figure 4.47: Displacement direction plot from FLAC for case (5)

4.6.3 Comparison

The same surface of failure obtained from limit equilibrium was depicted on the finite difference analysis of the slope shear strain increment in Figure 4.48.

Consistently, the result shows that the minimum values of factor of safety obtained from numerical analysis is equal to the minimum factor of safety value from limit equilibrium method. Although, the computed factor of safety was equal to limit equilibrium value, the failure surface is somewhat different. Moreover, the shape of failure plane seems to be circular for limit equilibrium method and non-circular for finite difference method showing sliding and overturning possible failure.

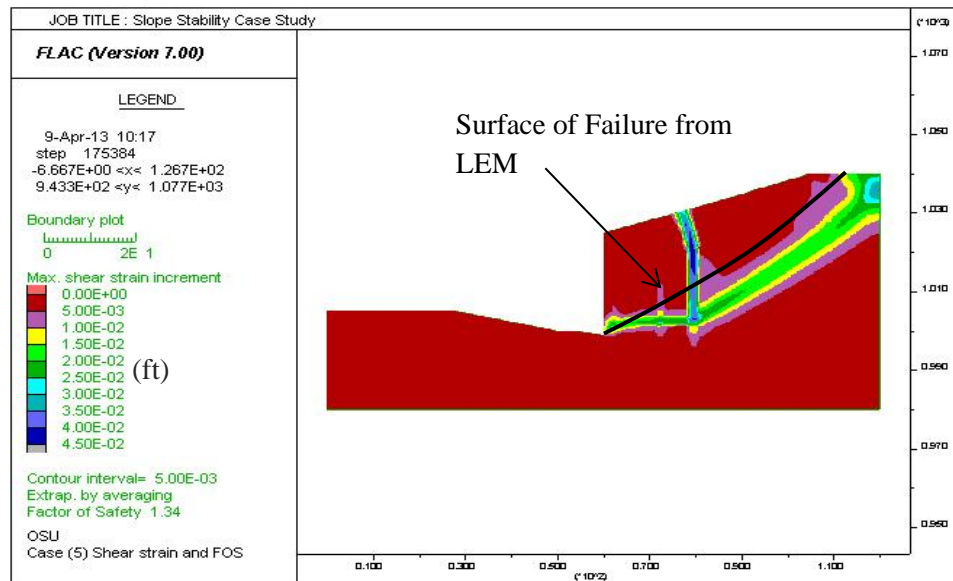


Figure 4.48: Critical surface from LEM depicted on shear strain from FDM for case (5)

CHAPTER V

5. SUMMARY AND CONCLUSIONS

5.1 Summary

The factor of safety of slope stability was determined by using the finite difference method in conjunction with the Shear Strength Reduction (SSR) technique and limit equilibrium method through Spencer's and Morgenstern-Price's methods which were explained in previous chapters. The primary focus of this research was to study: (a) the comparison of the factor of safety values from both methods, and (b) the failure mechanism of slopes by studying the surface of failure using both analyses. Five real cases were studied in this research as summarized below. Summary of results and findings are presented in Table 5.1.

Table 5.1: Factor of safety results for all cases and failure surface observation

Description	Factor of Safety			Failure surface observation
	Limit Equilibrium Method (LEM)	Finite Difference Method (FDM)	Difference in Percentage compare to FDM	
Case (1)	1.29 (with Spencer)	1.25	3% less than LEM	- Within the ring of max. shear strain - Circular for both methods
Case (2)	1.11 (with M-P*)	1.08	3% less than LEM	- Within the ring of max. shear strain - Non-circular for both methods
Case (3)	1.19 (with Spencer)	1.19	0%	- Slightly within the ring of max. shear strain - Circular for both methods
Case (4)	1.01 (with Spencer)	0.90	11% less than LEM	- Slightly out of the range of max. shear strain (Failure Cond.) - Non-circular for both methods
Case (5)	1.34 (with Spencer)	1.34	0%	- Out of the ring of max. shear strain - Non-circular for FD and circular for LE methods

*M-P: Morgenstern-Price Method

5.2 Conclusions

The following conclusions were developed based on the results presented in this research work.

- This study has illustrated that factor of safety analyses using limit equilibrium and finite difference methods can be expected to produce very similar results for both simple and complex slope cases. Previous studies by others have mostly used simplified slopes with homogeneous soils and simple geometry. However, this study included slopes with complex geometries, multiple soil layers including weak layers, reinforcing elements, retaining walls, seismic coefficients, and water surfaces. The close agreement between the two analysis methods indicates that the finite difference method can be used as a practical and meaningful verification of conventional limit equilibrium analyses of complex slopes.
- One important limitation of the conventional limit equilibrium method is that it requires an arbitrary selection of the search areas and shape of the potential failure surfaces prior to analyses. Accordingly, critical areas of the slope or critical shaped failure surfaces may be overlooked if the search areas and failure surface shapes are not well selected. The use of the finite difference method as a verification of traditional limit equilibrium methods is more ideal than using two different limit equilibrium programs to perform this verification since the location and shape of potential slip surfaces do not have to be defined in advance for the finite difference method.
- Either the finite difference method or finite element method may be used with the shear strength reduction technique to perform the verification analyses since both numerical methods use similar approaches and do not have the limitation discussed above for the limit equilibrium method. The numerical methods also have the incidental feature of

predicting deformations within the slope. This deformation aspect is important in evaluating the performance and acceptability of some slopes which are sensitive to movement. However, the limit equilibrium method does have certain advantages over the numerical methods as discussed below.

- The limit equilibrium method can be used to determine a factor of safety of a slope with a value significantly less than 1.0. While this is not meaningful for the actual factor of safety value at failure, it is meaningful for cases where reinforcing elements will be added later and the lower bound condition of the soil strength related to factor of safety is desired. The numerical methods essentially cannot be used to perform such an analysis since the strength reduction technique will not typically accommodate a failure condition with the factor of safety significantly below 1.0.
- The above discussion illustrates the great advantage of using both the limit equilibrium method and the finite difference (or finite element) method to mutually verify the slope analysis.

5.3 Recommendations

- Using more than one method for analysis of existing or proposed slopes is the best approach for achieving reliable results. The results of slope stability calculations should be independently checked, regardless of how the calculations are performed.
- The validity of the finite difference analysis and limit equilibrium results for both unreinforced and reinforced slopes have been compared; however, field data and more case studies are needed to provide more definitive results for a wider range of conditions.
- The finite difference prediction using the Mohr-Coulomb method was acceptable. However, it is recommended to use more cases and a laboratory testing program to further investigate the effectiveness and reliability of the method for a wider range of

conditions. Additional research using real slopes and actual case histories of complex slopes is needed.

- Future research should also include a comparison between the finite difference and finite element methods for factor of safety (strength reduction) analysis of slopes.

REFERENCES

- Bishop, A.W. (1955) The Use of the Slip Circle in the Stability Analysis of Slopes.
Géotechnique, London, England, Vol. 5, No. 1, pp. 7-17
- Budhu, M. (2000) *Soil Mechanics and Foundations*, First Edition, Johan Wiley & Sons, Inc,
University of Arizona, AZ
- Chen, W. R. (1995) *The Civil Engineering Handbook*. Editor-in-Chief, CRC Press, Inc.,
Boca Raton, FL
- Chang, Y. L. and Huang, T. K. (2005) Slope Stability Analysis Using Strength Reduction
Technique, *Journal of the Chinese Institute of Engineering*, Vol. 28, No. 2, pp. 231-240
- Cheng, Y. M. (2003) Location of critical failure surface and some further studies on slope
stability, *Computers and Geotechnics Journal*, No.30, pp. 255-267
- Cheng, Y. M., Lansivaara, T. and Wei, W. B. (2006) Two-dimensional slope stability analysis by
limit equilibrium and strength reduction methods, *Computers and Geotechnics Journal*, No.34,
pp. 137-150
- Cheng, Y. M., Lansivaara, T. and Wei, W. B. (2006) Factor of safety by limit equilibrium and
strength reduction methods, *Numerical Methods in Geotechnical Engineering*, pp. 485-490

- Dawson, E. M., Roth, W.H. and Drescher, A. (1999) Slope Stability Analysis by Strength Reduction. *Geotechnique*, Vol. 49, No. 6, pp. 835-840
- Diederichs, M. S., Lato, M., Hammah, R. and Quinn, P. (2007) Shear Strength Reduction (SSR) approach for slope stability analyses. *Taylor & Francis Group, London*, pp. 319-327
- Duncan, J.M. and Wright, S.G. (2005) *Soil Strength and Slope Stability*, John Wiley & Sons, Inc., Hoboken, NJ
- Duncan, J.M. (1996) State of art: limit equilibrium and finite-element analysis of slopes. *Journal of Geotechnical Engineering*, Vol. 122, No. 7, pp. 557-596
- Griffiths, D.V., and Lane P.A. (1999) Slope Stability Analysis by Finite Elements, *Geotechnique*, Vol. 49, No. 3, pp. 387-403
- Hammah, R., Yacoub T, Corkum, B., Curran, J. (2004) A Comparison of Finite Element slope stability Analysis with Conventional Limit-Equilibrium Investigation, *University of Toronto*.
- Holtz, R.D, and Kovacs, W.D. (1981) An Introduction to Geotechnical Engineering. *Prentice-Hall, Inc.* pp. 448
- Itasca Consulting Group Inc. (2011) FLAC - Fast Lagrangian Analysis of Continua, version 7.0, Fifth Edition
- Mendjel, D. and Messast, S. (2012) *Development of limit equilibrium method as optimization in slope stability analysis, structural Engineering and Mechanics*, Vol. 41, No. 3, pp. 339-348
- Morgenstern, N. R. and Price, V. E. (1965) The analysis of the stability of general slip surfaces, *Geotechnique*, Vol. 15, No.1, pp. 79-93
- Pourkhosravani, A. and Kalantari, B. (2011) A Review of Current Methods for Slope Stability Evaluation, *EJGE*, Vol. 16, pp. 1245-1254

Rocscience (2004) A New Era in Slope Stability Analysis: Shear Strength Reduction Finite Element Technique, *Article*

Spencer, E. (1967) A Method of Analysis of the Stability of Embankments Assuming Parallel Interslice Forces, *Géotechnique*, Vol. 17, No. 1, pp. 11-26

Terzaghi, K., Peck, R.B., and Mesri, G. (1996) *Soil Mechanics in Engineering Practice*. Third Edition, John Wiley & Sons, Inc. Article 18, pp. 135

U.S. Army Corps of Engineers, (2003) Engineer Manual. [Online] Available: <http://www.usace.army.mil/publications/eng-manuals>, (Accessed 02/15/2013)

Wanstreet, P. (2007) *Finite Element Analysis of Slope Stability*. Thesis presented to West Virginia University, at Morgantown, West Virginia, in partial fulfillment of the requirements for the degree of Master of Science

Wei, L., Koutnik, T., and Woodward, M. (2010) A slope Stability Case study by Limit Equilibrium and Finite Element Methods. *GeoFlorida 2010: Advance in Analysis, Modeling & Design*, pp. 3090-3099

Wei, W.B. and Cheng, Y.M. (2010) Soil nailed slope by strength reduction and limit equilibrium methods, *Computer and Geotechnics*, Vol. 37, pp. 602-618

VITA

Omar Ali M. Moudabel

Candidate for the Degree of

Master of Science

Thesis: SLOPE STABILITY CASE STUDY BY LIMIT EQUILIBRIUM AND
NUMERICAL METHODS

Major Field: Civil and Geotechnical Engineering

Biographical:

Education:

Completed the requirements for the Master of Science in Civil Engineering, Geotechnical Engineering at Oklahoma State University, Stillwater, Oklahoma in May, 2013.

Completed the requirements for the Bachelor of engineering in Civil Engineering, Structural Engineering at University of Tripoli, Tripoli, Libya in 1997.

Experience:

2011 – 2013: Graduate student and research Assistant, Oklahoma State University, USA.

2009 – 2010: Project manager Assistant, National Union Consultants, Libya.

2008 – 2009: Site Manager, EM-HIDROMANTAZA Company, Libya branch.

2006 – 2007: Construction engineer, BIWATER Company, Libya branch.

2002 – 2006: QA/QC offshore & offshore engineer, BESIX Company, Libya branch.

1998 – 2002: Site manager and QA/QC engineer, GMRA Company, Libya.

Professional Memberships:

Engineers' Union Membership, Tripoli, Libya.